Calibration Using ~~ng on~~ Downscaled and Bias-Corrected Satellite ~~Soil Moisture~~Soil-Moisture Data Can Improve Watershed Model ~~Performance in Predicting~~Representation of ~~Soil Moisture~~Soil-Moisture Variability

Binyam Workeye Asfaw[1], Siam Maksud[1], Daniel R. Fuka[1], Amy S. Collick[2], Robin R. White[3], Zachary M. Easton[1]

[1]Department of Biological Systems Engineering, Virginia Tech, Blacksburg, VA, USA

[2]Department of Agricultural Science, Morehead State University, Morehead, KY, USA

[3]School of Animal Sciences, Virginia Tech, Blacksburg, VA, USA

Correspondence to: Zachary M. Easton (zeaston@vt.edu)

Abstract

Watershed streamflow is often the focus of hydrological model calibration and evaluation, despite other potential objectives, including water quality management, flood protection, or agricultural management. When hydrological models are calibrated on streamflow, intermediate processes such as those affecting ~~soil moisture~~soil-moisture are not necessarily well represented. This research evaluated ~~the performance of downscaled and bias corrected soil moisture calibrated models against streamflow calibrated models both under single and multi-objective calibrations on field scale soil moisture estimation performance.~~whether calibration using downscaled and bias-corrected satellite soil-moisture improves prediction of field-scale soil-moisture relative to conventional streamflow-based calibration. In this work, downscaled satellite ~~soil moisture~~soil-moisture and streamflow data are used to calibrate a Soil and Water Assessment Tool – Variable Source Area model initialized using a terrain informed process to create hydrologic response units. In-situ ~~soil moisture~~soil-moisture measurements at 25 locations across a 4.2-ha mixed-grass pasture located in southwestern Virginia were used to estimate ~~field scale~~field-scale average ~~soil moisture~~soil-moisture variability for model evaluation. Leveraging downscaled satellite ~~soil moisture~~soil-moisture data substantially improved estimation of temporal ~~soil moisture~~soil-moisture variability without affecting the model streamflow performance. The multi-objective calibration using streamflow and satellite ~~soil moisture~~soil-moisture ~~improved overall model performance for both streamflow and soil moisture~~soil-moisture improved soil-moisture performance while maintaining streamflow performance comparable to streamflow-only calibration. These results demonstrate the potential for satellite ~~soil moisture~~soil-moisture–informed calibration to improve internal hydrologic state estimation in small, saturation excess watersheds. Furthermore, these results highlight the importance of coupling statistical performance gains

with evaluation of hydrologic realism when extending such approaches to broader modeling applications.

1 INTRODUCTION

Hydrological model calibration is most commonly performed using streamflow observations because they are widely available and integrate catchment-scale water balance behavior (Pechlivanidis et al., 2011). However, calibration based solely on streamflow can leave internal states and fluxes, particularly ~~soil moisture~~soil-moisture, poorly constrained, despite their central role in governing evapotranspiration, runoff generation, and hydrologic connectivity (Brocca et al., 2017). Inadequate representation of ~~soil moisture~~soil-moisture therefore limits model usefulness for applications such as agricultural management, water quality assessment, and interpretation of vadoze zone process-level behavior.

Direct characterization of watershed-scale ~~soil moisture~~soil-moisture is challenging due to strong spatial heterogeneity and the cost of dense monitoring networks (Brocca et al., 2010; Vereecken et al., 2015). Satellite-based ~~soil moisture~~soil-moisture products therefore provide an attractive alternative, offering spatially continuous observations that can complement traditional calibration targets. Products derived from missions such as Soil Moisture Active Passive (SMAP) (Colliander et al., 2017; O'Neill et al., 2018)~~)~~, Soil Moisture and Ocean Salinity (SMOS) (Kundu et al., 2017), Advanced Scatterometer (ASCAT) (H SAF, 2021), and Advanced Microwave Scanning Radiometer 2 (AMSR2) (Cho et al., 2015) have been increasingly incorporated into hydrological model calibration and data assimilation frameworks (Brocca et al., 2017). Reported outcomes, however, are mixed. Some studies show improved model streamflow or drought estimation performance (Azimi et al., 2020; De Santis et al., 2021; Nanda et al., 2023; Patil & Ramsankaran, 2017; Sun, 2016; Wakigari & Leconte, 2023), while others report improved ~~soil moisture~~soil-moisture simulation with little or no degradation streamflow performance (Rajib et al., 2016; Dangol et al., 2023; Duethmann et al., 2022; López et al. 2017). These trade-offs reflect differences in ~~watershed scale~~watershed-scale, dominant runoff mechanisms, satellite sensing depth, preprocessing approaches, and model structure.

Uncertainty in ~~soil moisture~~soil-moisture observation/estimation is particularly pronounced in small, saturation-excess–dominated watersheds, where runoff generation depends strongly on antecedent root zone ~~soil moisture~~soil-moisture storage, topographic convergence, and hydrologic connectivity (Beven et al. 2021; Easton et al., 2008; Lyon et al., 2004). In such settings, coarse-resolution satellite ~~soil moisture~~soil-moisture products, both native and downscaled, may capture large scale temporal dynamics but fail to represent event-scale wetness organization critical for runoff initiation (Gomis-Cebolla et al., 2022; Duethmann et al., 2022). Moreover, many previous studies are conducted in large basins (>700 km²), with comparatively few demonstrations in smaller basins (Duethmann et al., 2022; Dangol et al., 2023) and most lack independent evaluation of internal state estimates against field observations, limiting insight into whether calibration improvements reflect physical realism or compensatory parameter behavior. In addition, few studies report the effect of incorporating satellite ~~soil moisture~~soil-moisture products for model calibration on both ~~soil moisture~~soil-moisture and streamflow estimation performance (Dangol et al., 2023; Eini et al., 2023; Rajib et al., 2016). While there is agreement that remotely sensed ~~soil moisture~~soil-moisture can be used to calibrate a watershed model for improved ~~soil moisture~~soil-moisture estimation, the scale of ~~soil moisture~~soil-moisture outputs is still coarse (> 2km^2), and additional effort is required to inform field-scale management applications (Mascaro et al., 2011).

Watershed models play a critical role in translating spatially continuous, remotely sensed observations into ~~field scale~~field-scale predictions of hydrologic states and processes. Their utility depends not only on the availability of satellite data, but on whether model structure can realistically map those observations onto the dominant controls governing runoff generation and ~~soil moisture~~soil-moisture variability. The Soil and Water Assessment Tool (SWAT) Variable Source Area (VSA) model (SWAT-VSA) provides a targeted framework for evaluating satellite-informed calibration in saturation-excess environments. By redistributing soil and hydrologic properties according to topographic index (TI) classes, SWAT-VSA improves representation of spatial saturation patterns and runoff source areas relative to conventional hydrologic response unit (HRU) definitions (Easton et al., 2008; Fuka et al., 2016). This structure also supports scale-consistent evaluation of modeled ~~soil moisture~~soil-moisture using TI-weighted aggregation of field measurements, helping bridge the gap between point observations, satellite products, and model states.

In this study, we evaluate whether downscaled and empirically bias corrected satellite ~~soil moisture~~soil-moisture product ~~data~~ can improve internal hydrologic state estimation in a small (~14.5 km²), saturation excess dominated watershed using SWAT-VSA. We contrast three calibration strategies: (i) streamflow only, (ii) ~~soil moisture~~soil-moisture only, and (iii) ~~multi objective~~multi-objective calibration using both streamflow and satellite ~~soil moisture~~soil-moisture. Model performance is evaluated using both conventional goodness of fit statistics, as well as through ~~independent~~comparison against ~~field scale~~field-scale ~~soil moisture~~soil-moisture measurements collected across a 4.2 ha monitoring field and aggregated using TI-based weighting consistent with the model structure (Easton et al., 2008; Asfaw et al., 2025).

The objectives were to test whether satellite ~~soil moisture~~soil-moisture informed calibration improves temporal ~~soil moisture~~soil-moisture variability without degrading streamflow performance, and whether multi-objective calibration can balance predictive accuracy with hydrologic realism. By combining downscaled satellite ~~soil moisture~~soil-moisture, terrain informed model structure, and independent field evaluation, this work advances understanding of when and how satellite ~~soil moisture~~soil-moisture can meaningfully constrain watershed model parameters in small, ~~terrain controlled~~terrain-controlled catchments.

2 MATERIAL AND METHODS

2.1 Study Area

The study was conducted in the upper Stroubles Creek watershed, Montgomery County, Virginia, USA. Streamflow was measured at the Virginia Tech StREAM (Stream Research, Education and Management) Lab monitoring station (Hofmeister et al., 2015), which drains a 14.5 km² headwater watershed within the Valley and Ridge physiographic region. The watershed is-characterized by dolomite and limestone geology with springs and sink holes (Ketabchy, 2018; Parece et al., 2010). The climate is humid, temperate, receiving 1200 mm annual precipitation of which 760 mm is subject to evapotranspiration (Ketabchy, 2018; Asfaw et al., 2025). The watershed has 67% pervious and 32% impervious land cover (Nayeb Yazdi et al., 2019).

The watershed is strongly saturation excess dominated (Asfaw et al., 2025), with runoff generation controlled by topography and shallow soil storage, making it well suited for evaluation of VSA hydrology and satellite ~~soil moisture~~soil-moisture informed calibration.

2.2 ~~Soil Moisture~~Soil-Moisture Data

2.2.1 Soil Moisture Active Passive (SMAP) ~~Soil Moisture~~Soil-Moisture and Downscaling

SMAP is a global surface ~~soil moisture~~soil-moisture acquisition mission at 36 km resolution (Entekhabi et al., 2014; O’Neill et al., 2023), using an L-band radiometer and L-band radar.

Several approaches were used to post-process and increase SMAP product resolution for different applications (Abbaszadeh et al., 2021, Chan et al., 2018; Das et al., 2018;). Among such efforts was the National Aeronautics and Space Administration (NASA) and the United States Department of Agriculture (USDA) Enhanced SMAP 10 km resolution product, generated by incorporating SMAP data using Kalman Filter into the Modified Palmer Two-Layer ~~soil moisture~~soil-moisture model (Mladenova et al., 2020).

In this study, satellite ~~soil moisture~~soil-moisture derived from the Enhanced SMAP product and downscaled to 500 m resolution using a machine learning tool, the ‘mlhrsm’ package in R (Peng et al., 2024), was used. The downscaling applies a pretrained quantile random forest model that uses multi-sensor predictors including Sentinel-1 backscatter, MODIS land surface temperature, Landsat-derived vegetation indices (surface reflectance, NDVI and NDWI), a 10 m USGS digital elevation model (DEM), POLARIS soil properties (clay, sand and bulk density), and NLCD land-cover classes.

The downscaling model outputs daily volumetric ~~soil moisture~~soil-moisture estimates (m^3 m^{-3}) for each 500 m cell intersecting the watershed for the period April 2015 to August 2022. The downscaled ~~soil moisture~~soil-moisture was spatially averaged across the watershed to generate a daily watershed mean ~~soil moisture~~soil-moisture time series used for model calibration.

2.2.2 In-S~~s~~itu ~~Soil Moisture~~Soil-Moisture

In-situ ~~soil moisture~~soil-moisture measurements were collected on 20 sampling dates between March 2023 and January 2024 at 25 locations within a 4.2 ha mixed-grass pasture located inside the watershed. Sampling locations were distributed across the field covering the full range of terrain classes present. Measurements were collected 1–3 days following precipitation events to capture ~~soil moisture~~soil-moisture conditions ranging from near wilting point to near saturation (0.15–0.45 m^3 m^{-3}).

Mean ~~field scale~~field-scale ~~soil moisture~~soil-moisture was calculated using TI class weighted aggregation, consistent with the SWAT-VSA HRU structure. Point measurements were first grouped by TI class and then aggregated to a ~~field scale~~field-scale mean using the relative areal coverage of each TI class within the monitoring field. Although the monitored field represents a small fraction of the watershed, previous studies in similar saturation excess system show that spatial ~~soil moisture~~soil-moisture variability is primarily governed by topographic controls rather than localized soil heterogeneity (Easton et al., 2008; Lyon et al., 2004; Asfaw et al., 2025). While land use and soil variability contribute to ~~watershed scale~~watershed-scale moisture patterns, the small size of the watershed supports the assumption of near uniform precipitation and evapotranspiration inputs, reducing the likelihood that climatic gradients confound field to watershed comparisons. Furthermore, previous work in the study area shows that spatial ~~soil moisture~~soil-moisture differences are dominated by topographic effects rather than local soil variation effects (Asfaw et al., 2025).

The temporal variability of ~~soil moisture~~soil-moisture was well represented in the data with observations occurring on days near to the soil permanent wilting point and saturated ~~soil moisture~~soil-moisture conditions (0.15 – 0.45 volumetric water content). Calculated ~~field scale~~field-scale average ~~soil moisture~~soil-moisture was used for model performance evaluation across the same domain. Additional details on this dataset are reported in Asfaw et al. (2025).

2.3 SWAT-VSA model

The SWAT model is a semi distributed, ~~watershed scale~~watershed-scale hydrologic and water quality model that simulates the water balance, surface runoff, subsurface flow, and associated sediment and nutrient transport using land use, soil, management, weather, and topographic inputs (Neitsch et al., 2009). SWAT-VSA is a modification to SWAT designed to represent VSA hydrology which is characteristic of saturation excess dominated landscapes (Easton et al., 2008).

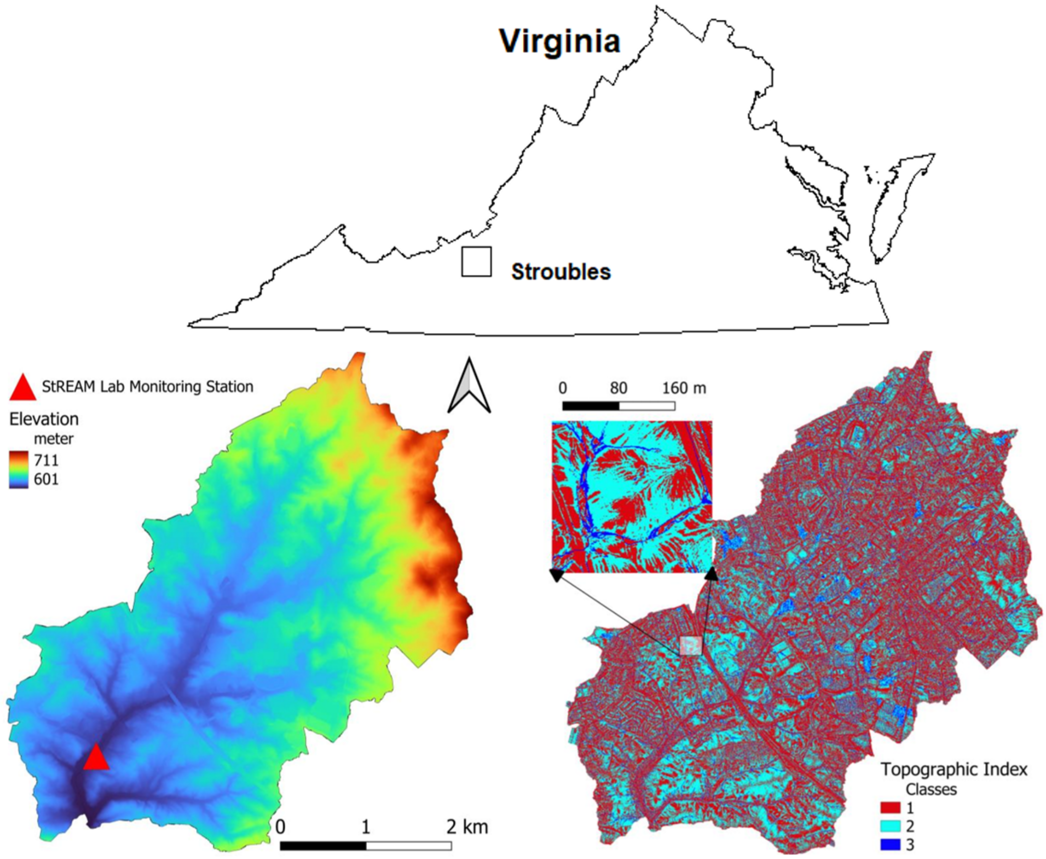

Figure 1: Location map of the Stroubles Creek watershed (top), digital elevation model (left) and Topographic Index Class (right; magnified view of 4.2 ha pasture field inset).

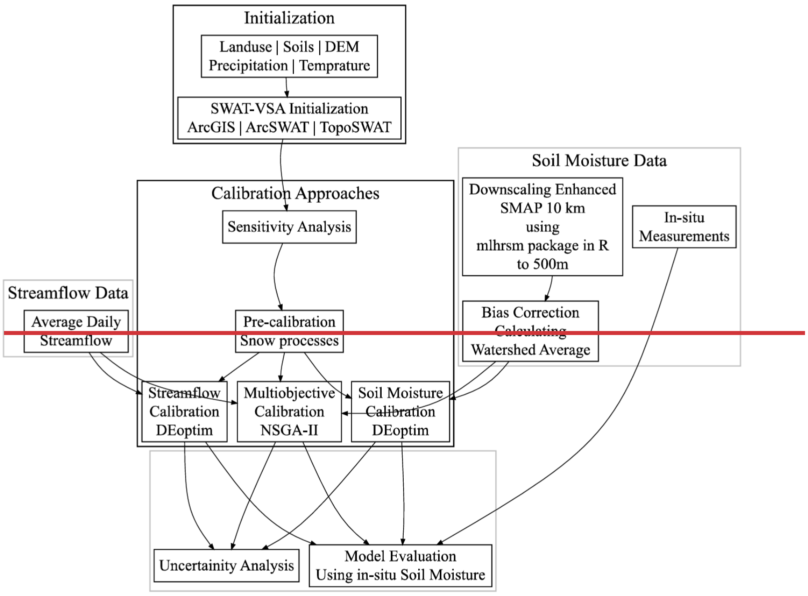

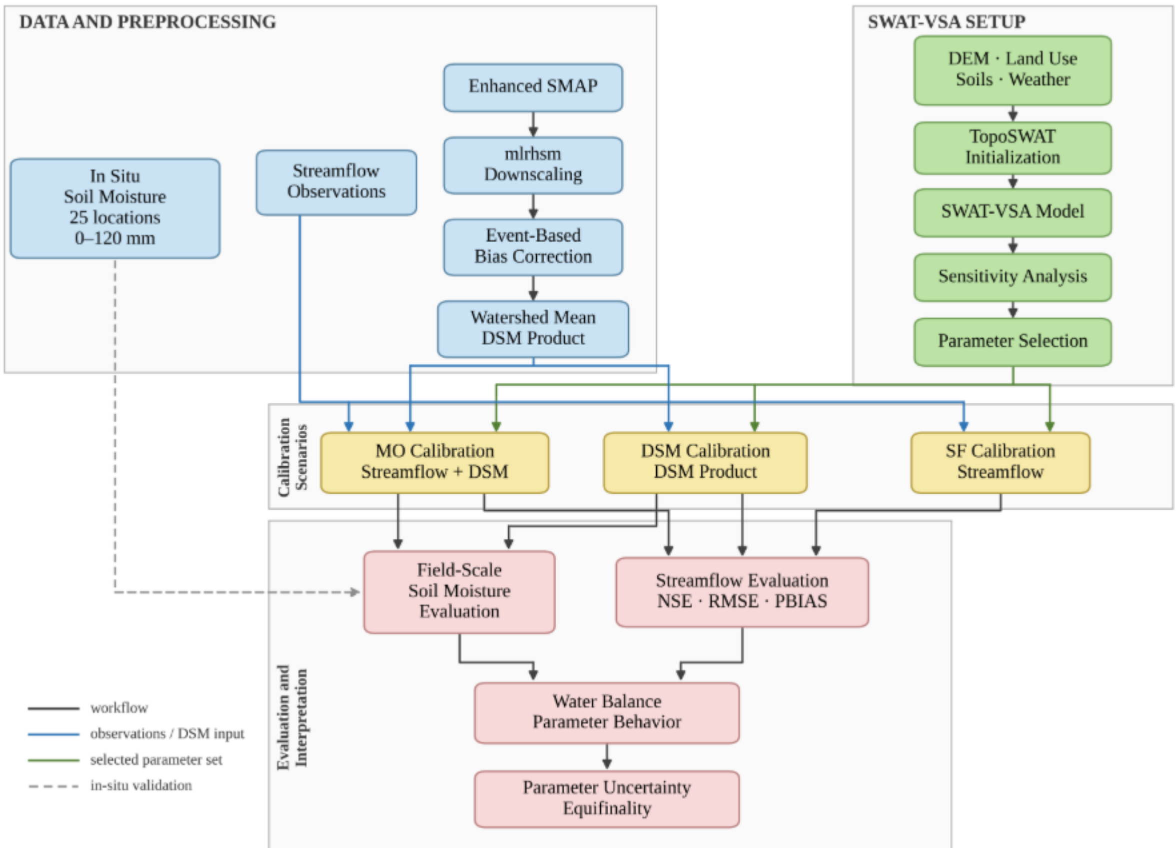

Figure 2: ~~Workflow of data processing, model calibration, and model performance evaluation.~~ Study workflow showing generation of the downscaled and bias-corrected

soil-moisture product (DSM), SWAT-VSA setup, calibration, evaluation, and uncertainty analysis. Three calibration approaches were compared: streamflow-only (SF), soil-moisture-only (DSM), and multi-objective (MO). Streamflow and field-scale in-situ soil-moisture observations were used to assess model performance and interpret parameter behavior and equifinality.

In SWAT-VSA, the curve number (CN) based runoff formulation is adapted to continuously redistribute watershed average ~~soil moisture~~soil-moisture storage as a function of topographic index (TI), thereby linking runoff generation to ~~terrain controlled~~terrain-controlled wetness patterns (Easton et al., 2008; Fuka et al., 2016). TI values together with soil and land use information are used to define HRUs, which consequently represent spatial variability in runoff generation and ~~soil moisture~~soil-moisture state. SWAT computes the soil water content for each layer individually at a daily time step. Infiltration to the surface layer is calculated after subtracting evaporative demand and surface runoff from precipitation at a daily time step. Vertical drainage of excess soil water is simulated as percolation, while ~~soil moisture~~soil-moisture depletion under unsaturated conditions occurs through plant uptake and transpiration and soil water evaporation from the soil layers. These unsaturated zone processes are influenced by the plant evapotranspiration compensation factor (EPCO) and soil evaporation compensation factor (ESCO) parameters, which are commonly adjusted during calibration to regulate vertical moisture redistribution. Within each soil layer, SWAT assumes homogeneous moisture distribution~~,~~. When the model soil layer ~~are~~is thick, this assumption can dampen simulated moisture variability in surface soil layers and complicate comparison with surface sensitive satellite products and shallow in-situ measurements. To enable depth~~-~~-consistent comparison among modeled, satellite derived, and in-situ ~~soil moisture~~soil-moisture, the SWAT soil profile was modified to explicitly simulate the 0-50 mm and 50-120 mm layers in addition to standard profile. Reported soil water content was converted from depth units to volumetric water content adjusted relative to the permanent wilting point for the dominant soil in the watershed. This modification improves ~~representation~~the representation of near surface wetting and drying cycles and facilitates direct comparison across data sources.

2.3.1 Model Initialization

The SWAT-VSA model initialization was performed using ArcSWAT version 2012.10_8.26 in ArcGIS Desktop 10.8.2. The 2019 land use data were retrieved from the US Geologic Survey (USGS) National Land Cover Data (NLDC) website using the ‘get_nlcd’ function from ‘FedData’ package in R (Bocinsky et al., 2025; Jin et al., 2023). The USGS 3DEP program 1m resolution elevation data were used for watershed delineation, estimation of slope, and calculation of TI.

The VSA initialization was executed using TopoSWAT (Fuka & Easton, 2016), an ArcGIS plugin. The plugin was modified to enable generation of three TI classes ~~generation~~ from Asfaw et al. (2025). Using Natural Breaks from Spatial Analyst in Arc GIS, TI values were grouped into each class minimizing variance within class and maximizing variance among classes. The three TI classes from class 3 to 1 cover 6%, 38%, and 56% of the watershed area, respectively. Soils data were collected from the FAO-UNESCO Digital Soil Map (FAO, 2007). TopoSWAT downscales soil texture, soil depth, available water capacity, and hydraulic conductivity across TI classes. This was demonstrated to improve spatial representation of soil properties in VSA dominated watersheds (Fuka et al., 2016; Collick et al., 2015). Weather data from the Global Historical Climatology Network (GHCN) were used for model forcing. The data were acquired using the ‘FillMissWX’ function in R (Garna et al., 2023).

2.4 Data for Model Calibration and Evaluation

2.4.1 Streamflow Data

The StREAM lab monitoring station collects stage readings at a frequency of 10-15 minutes. Model calibration and evaluation were performed at a daily timestep. Stage was converted to discharge using a ~~site specific~~site-specific rating curve and aggregated to daily mean streamflow values using the zoo package in R (Zeileis et al., 2025). D~~-~~aily values were excluded if more than 12 hours or more of data were missing. The resulting streamflow record extended from 2011 to 2024. The data for years 2011 and 2012 were excluded due to extended periods of missing values. The period January 2013 – December 2021 was used for model calibration, and January 2022 - May 2024 were reserved for model evaluation. The streamflow data also provides an independent data source for model evaluation when calibrating ~~soil moisture~~soil-moisture.

2.4.2 ~~Soil Moisture~~Soil-~~-m~~Moisture

The downscaled, 500 m resolution~~,~~ ~~soil moisture~~soil-moisture product was spatially averaged across the watershed to generate a daily watershed-mean ~~soil moisture~~soil-moisture time series for calibration. Downscaling was required because the native 10 km Enhanced SMAP resolution is far larger than the 14.5 km² watershed. The 500 m downscaled product constrains the satellite signal to the watershed boundary and improves temporal representativeness at the scale of interest.

These spatio-temporal improvements are needed to constrain ~~soil moisture~~soil-moisture~~-~~-related model parameters at the ~~watershed scale~~watershed-scale. The choice of 500 m resolution was also constrained by the available pretrained models in the mlhrsm downscaling package, which does not currently provide alternative target resolutions.

Importantly, spatial averaging of the downscaled ~~soil moisture~~soil-moisture fields does not undermine the value of using the SWAT-VSA model. SWAT-VSA relies on ~~TI~~ -~~base~~TI-based ~~d~~ HRUs to represent spatial patterns of saturation and runoff generation. While calibration uses a ~~watershed scale~~watershed-scale ~~soil moisture~~soil-moisture time series, the model internally maintains spatially explicit hydrologic processes using TI classes. HRU weighted aggregation ensures that model predicted ~~soil moisture~~soil-moisture is scaled to the watershed or field boundary in a manner consistent with the model's internal hydrologic structure.

Following initial comparison with in-situ measurements, the downscaled satellite ~~soil moisture~~soil- moisture exhibited a narrower dynamic range and attenuated peak wetness relative to observed ~~soil moisture~~soil- moisture in the monitoring field (maximum ~32% versus ~45% volumetric water content) To address this limitation, a simple event-~~-~~based ~~bias correction~~bias-correction was applied at the ~~watershed scale~~watershed- scale for days with substantial effective precipitation, Eq. 1. The corrected ~~soil moisture~~soil- moisture, $\theta_{s,cor}$, was calculated as:

$$\theta_{s,cor} = \begin{cases} \theta_s + k\sigma & if\ dP \geq d \\ \theta_s & if\ dP < d \end{cases} \qquad \text{(Eq. 1)}$$

where $\theta_{s,cor}$ is the watershed mean downscaled and bias corrected ~~soil moisture~~soil–moisture, σ is average standard deviation of the uncertainty bound around the downscaled mean ~~soil moisture~~soil-moisture estimates from the mlhrsm, θ_s is the average downscaled watershed ~~soil moisture~~soil–moisture, k is a scaling factor, and d is a threshold effective precipitation depth in mm calculated as equivalent value to bring the ~~top 120~~ 0-50 ~~-~~-mm soil layer from field capacity to saturation. This depth corresponds to the soil layer represented by the satellite soil-moisture product and used in model calibration. A second derived soil layer was also calculated: the 0–120 mm composite soil-moisture layer was used only for independent evaluation against field observations.

A three-day rolling mean was applied following ~~bias correction~~bias-correction. In-situ ~~soil moisture~~soil-moisture observations were not used in the derivation of the bias-correction parameters. However, they were considered when selecting among Pareto-equivalent solutions and therefore should be viewed as an auxiliary model-selection criterion rather than a fully independent validation dataset (Table A1).

Although calibration uses the downscaled and bias~~-~~-corrected satellite ~~soil moisture~~soil-moisture data, ~~all~~ model evaluation is performed using independent observations not involved in preprocessing or calibration. In particular, in-situ ~~soil moisture~~soil-moisture measurements collected at 25 locations within the 4.2-ha field (0–120 mm depth) were used exclusively for model evaluation, not for calibration, providing an independent benchmark for ~~field scale~~field-scale ~~soil moisture~~soil-moisture dynamics. All calibration analyses hereafter refer to the watershed average bias-corrected soil-moisture time series unless otherwise noted.

~~To ensure consistent comparison across data sources, soil moisture depths were aligned between satellite estimates, model outputs, and in-situ measurements. The 0–50 mm SWAT soil layer was used for calibration against the satellite soil moisture series, while a 0–120 mm composite layer was reserved for evaluation against field measurements (Table A1). All calibration analyses hereafter refer to the watershed average bias corrected soil moisture time series unless otherwise noted.~~

~~The downscaled, watershed average, and bias-corrected data were used for model calibration. From here forward, these data are referred to simply as soil moisture data for brevity.~~

2.4.3 Bias-Correction Rationale and Procedure

An event~~-~~-based ~~bias correction~~bias-correction was applied to the watershed average downscaled ~~soil moisture~~soil-moisture series to enhance short term wetting responses while preserving the long~~-~~-term temporal structure. The correction (Eq. 1), is triggered when daily effective precipitation exceeds a threshold of 5 mm, representing the depth, d, required to fill the soil layer from field capacity to saturation over the top 0–50 mm. When triggered, the downscaled ~~soil moisture~~soil-moisture estimate is increased by a multiple (k) of the model reported uncertainty (σ), where σ is the standard deviation around the downscaled mean returned by the mlhrsm quantile random forest model.

This approach selectively expands peak ~~soil moisture~~soil-moisture responses during hydrologically important events, addressing the observed attenuation of wetness extremes in the uncorrected downscaled product while leaving dry period behavior and long term means unchanged. The precipitation threshold reflects the shallow storage deficit that must be overcome before saturation excess runoff responses emerge in topographically organized landscapes.

In situ ~~soil moisture~~soil-moisture observations were not used to derive or calibrate the ~~bias correction~~bias-correction parameters (σ, k, or d). Instead, σ is provided directly by the downscaling model, d is estimated from soil hydraulic properties and target depth, and k is set a priori for parsimony. In-situ measurements are used only for independent model evaluation and to qualitatively confirm that the corrected ~~soil moisture~~soil-moisture series exhibits a physically realistic range of wetness.

2.5 Model Calibration

2.5.1 Model Sensitivity

To identify the most influential parameters for calibration of the SWAT-VSA model, a sensitivity analysis was performed. A total of 20 parameters relevant to streamflow generation and soil-moisture dynamics were evaluated using relative sensitivity based on changes in Nash-Sutcliffe Efficiency (NSE) (Nash & Sutcliffe, 1970) from January 1, 2015, through December 31, 2019. Table 1 provides the tested parameters, and their rank based on relative sensitivity values. Because the sensitivity analysis was based on streamflow NSE, parameters that primarily influence soil-moisture dynamics may be underrepresented in the resulting rankings. However, all parameters with known relevance to soil-water storage and redistribution were retained for calibration.

2.5.2 Calibration Strategy

Model calibration targeted daily streamflow and watershed average ~~soil moisture~~soil-moisture in the top 0-50 mm soil layer. Three calibration approaches were included: 1) streamflow only, 2) ~~soil moisture~~soil -moisture only, and 3) a multi-objective calibration using both streamflow and ~~soil moisture~~soil-moisture data. Prior to calibrations, baseflow and snow processes were pre-calibrated following a stepwise calibration approach to constrain parameter ranges. Snow parameters were subsequently held constant as initial analysis indicated the values provide adequate representation of snow processes. Baseflow separation was performed using the ’baseflowseparation’ function from EcoHydRology package (Fuka et al., 2013; Nathan & McMahon, 1990). Table 1 provides the calibrated parameters and their ranges for each method.

Single-objective model calibrations were performed using a differential evolutionary algorithm, an exhaustive parameter space search using the ‘DEoptim’ R package (Mullen et al., 2011). Thirteen parameter vectors were evaluated per generation over 50 generations, for a total of 650 parameter vectors. Fifty generations w~~as~~ere deemed sufficient after monitoring the successive diminishing returns in objective function minimization. The multi-objective calibration was performed using non-dominated sorting genetic algorithm (NSGAII) for the pareto front solution (Bek~~-~~ele & Nicklow, 2007; Deb et al., 2000) implemented using the

Python library ‘pymoo’ (Blank & Deb, 2020). Among pareto-optimal solutions, final model selection additionally considered skill in reproducing field-scale in-situ ~~soil moisture~~soil-moisture observations. The VSA implementation employed three TI classes representing progressively wetter landscape positions. The CN2 parameter (curve number for~~ the~~ average ~~soil moisture~~soil-moisture conditions)~~,~~ was used to estimate the watershed average moisture storage deficit S and redistributed across TI classes following the relationship developed in Easton et al. (2008). CN2 values for individual HRUs were updated at each calibration iteration based on the optimized watershed-average CN2. Initial CN2 estimates were derived using a water-balance approach (Lyon et al. 2004), with subsequent adjustment governed by the optimization algorithm.

2.5.3 Goodness of Fit Measures

Model performance was evaluated using the coefficient of determination (R2), the root mean squared error (RMSE), the percent bias (PBIAS), and the Nash-Sutcliffe efficiency (NSE) (Krause et al., 2005; Moriasi et al., 2007). Streamflow calibration sought to maximize the NSE value as this is the most widely used approach. For ~~soil moisture~~soil-moisture, the RMSE was used due to the bounded range, lower variance, and longer memory of soil-moisture time series, for which NSE can be overly sensitive to small errors (Entekhabi et al., 2010; Krause et al., 2005).

2.5.4 Parameter Uncertainty

Parameter uncertainty was quantified using the parameter sets developed during model calibration that satisfied performance thresholds of NSE $\geq$ 0.5 for streamflow, RMSE $\leq$ 0.05 $m^3\ m^{-3}$ for ~~soil moisture~~soil- moisture, or both. The extent of parameter uncertainty associated with each parameter was then scaled from 0-100 using the initial parameter range and the equation given below. Normalized parameter uncertainty (Pn) provides an equal scale for comparison across parameters (Kumar & Merwade, (2009) and Rajib & Merwade, (2016):

$$P_n = \left(\frac{P_O - R_{min}}{R_{max} - R_{min}}\right) * 100 \qquad (2)$$

where, P_n is the normalized parameter uncertainty, P_o is parameter value from parameters vectors which fulfilled the selection criteria, and $R_{min/max}$ are initial parameter ranges.

3 RESULTS

Table 1 summarizes parameter sensitivity and calibrated values across the three calibration approaches. The soil depth parameter was not calibrated but rather was adjusted during the model initialization to ensure equivalent comparison between observed and simulated ~~soil moisture~~soil- moisture (Table 1). During calibration, the curve number parameter (CN2) was updated at each iteration by redistributing the watershed-average storage deficit across hydrologic response units according to TI classes following Easton et al. (2008).

Parameters controlling runoff generation and ~~soil moisture~~soil-moisture dynamics (CN2, Bulk Density, Available Water Content (AWC), ESCO, Saturated Hydraulic Conductivity (Ksat), EPCO) in Table 1, were found to be influential across calibration approaches, while parameters controlling baseflow were less influential. Calibrated CN2 and bulk density parameters were similar across calibration approaches, while AWC, ESCO, Ksat and EPCO differed substantially, reflecting contrasting calibration targets.

Table 1: Model parameter sensitivity rank, initial range, and calibrated values.

Parameter	Description	Method	Range		§ SR	¶ Calibrated value		
			min	max		SF	DSM	MO
CN2	Runoff curve number of moisture condition II	replace	40	70	1	42.0	46.7	41.4
Depth	Soil depth	multiply	0.3	3	2	† NC	† NC	† NC

Bulk Density	Soil bulk density	multiply	0.5	1.5	3	0.93	1.22	1.13
‡ SMFMN	Snow melt factor minimum	replace	0	5	4	4.50	4.50	4.50
AWC	Available water content	multiply	0.3	3	5	2.55	1.5	2.70
‡ SMFMX	Snow melt factor maximum	replace	0	5	6	4.50	4.50	4.50
ESCO	Soil evaporation compensation factor	replace	0.1	1	7	0.11	0.69	0.34
Ksat	Saturated hydraulic conductivity	multiply	0.3	3	8	2.36	1.55	2.92
EPCO	Plant evaporation compensation factor	replace	0	1	9	0.94	0.77	0.85
‡ TIMP	Snowpack temperature lag factor	replace	0.01	1	10	0.01	0.01	0.01
‡ SFTMP	Snow fall temperature	replace	-5	5	11	4.00	4.00	4.00
‡ SMTMP	Snow melt temperature	replace	-5	5	12	2.00	2.00	2.00
GW_DELAY	Ground water delay (days)	replace	1	7	13	5.85	3.59	5.30
ALPHA_BF	Baseflow alpha factor (days)	replace	0.12	0.30	14	0.25	0.18	0.26
GWQMN	Threshold depth of water in the shallow aquifer required for return flow initiation (mm)	replace	10	500	15	417	213	494
GW_REVAP	Groundwater “revap” coefficient	replace	0.01	0.05	16	0.04	0.03	0.05
REVAPMN	Threshold depth of water in the shallow aquifer for “revap” initiation (mm)	replace	500	1000	17	996	813	649
RCHRG_DP	Recharges to deep aquifer (fraction)	replace	0.25	0.35	18	0.34	0.33	0.32
SURLAG	Surface runoff lag coefficient	replace	0	15	19	5.15	3.3	4.5

† Not Calibrated
‡ Pre-calibrated snow processes parameter values are underlined
§ Sensitivity Ranking (SR), using streamflow as the target variable

¶ Calibration on streamflow (SF); Calibration on ~~soil moisture~~soil-moisture (DSM); Calibration multi-objective (MO)

3.1 Comparison of Downscaled and Bias-Corrected ~~Soil Moisture~~Soil-Moisture Products

To evaluate how ~~bias correction~~bias-correction alters the ~~soil moisture~~soil-moisture signal used for calibration, two products were compared at the ~~watershed scale~~watershed-scale: (1) the 500-m downscaled ~~soil moisture~~soil-moisture series generated using the mlhrsm pretrained quantile random forest model, and (2) the bias corrected downscaled product used in model calibration. The uncorrected downscaled ~~soil moisture~~soil-moisture product exhibits a reduced dynamic range and underrepresents peak wetness relative to in-situ observations, as indicated by comparison with field observations presented in Section 3.3.2. Following ~~bias correction~~bias-correction, the ~~soil moisture~~soil-moisture product exhibits increased peak responses immediately following precipitation events, ~~and improved temporal agreement with in-situ measurements~~ and a greater dynamic range (Fig. 3). Comparison statistics against the independent field observations are presented in Fig. 6

The ~~bias correction~~bias-correction primarily affects wet-period responses while the lower envelope of the ~~soil moisture~~soil-moisture signal remains unchanged, confirming that the procedure enhances event responsiveness without artificially shifting long-term trends.

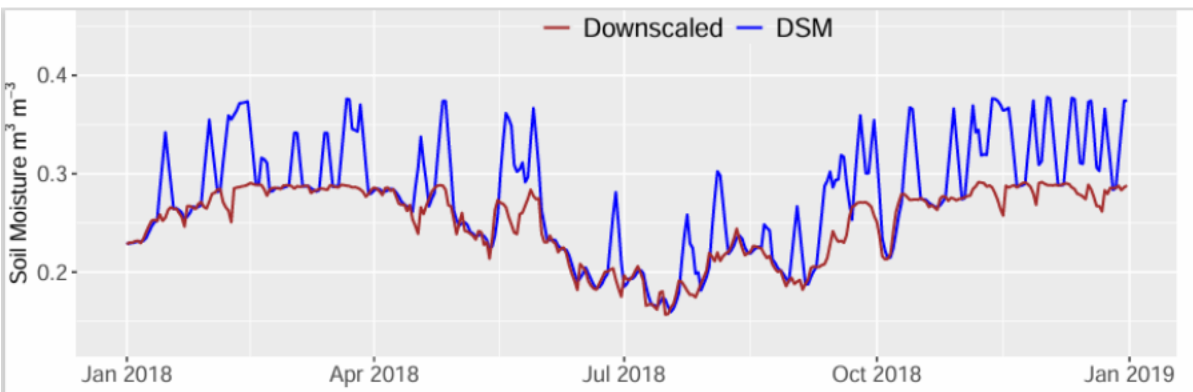

Figure 3: Time series of downscaled (mlhrsm product) and downscaled-bias-corrected ~~soil~~

~~moisture~~soil-moisture (DSM) at the ~~watershed scale~~watershed-scale. ~~Only d~~Data from only one year are shown for clarity.

3.2 Streamflow Estimation Performance

The three calibration approaches produced comparable streamflow estimation performance during the calibration period, with slightly lower performance for the ~~soil moisture~~soil-moisture calibrated model. Calibration targeting streamflow resulted in NSE, RMSE, and PBIAS values of 0.58, 0.32, -4.1%, respectively (Fig. 4). The multi-objective calibration, optimizing both streamflow and ~~soil moisture~~soil-moisture, achieved identical NSE and RMSE values (0.58 and 0.32 $m^3 s^{-1}$), with a more negative PBIAS (-10.7%), indicating increased underestimation bias. The ~~soil moisture~~soil-moisture calibration was not optimized for streamflow but nonetheless reproduced daily streamflow dynamics with an NSE of 0.54, RMSE of 0.33 $m^3 s^{-1}$, and PBIAS of 28.7% (Fig. 4), reflecting a consistent overestimation bias. Both the streamflow and multi-objective calibrated models reproduced baseflow magnitude and the timing of high-flow events, although peak flows were occasionally underestimated, particularly for the multi-objective calibration. In contrast, the ~~soil moisture~~soil-moisture calibrated model exhibited systematic overestimation of low flows (Fig. A1), reflected in the positive streamflow bias.

3.3 ~~Soil Moisture~~Soil-Moisture Estimation Performance

3.3.1 Calibration-~~s~~Scale ~~Soil Moisture~~Soil-Moisture (Satellite)

When evaluated against the bias corrected downscaled ~~soil moisture~~soil-moisture calibration target, the streamflow-calibrated model resulted in RMSE, R^2, and NSE values of 0.07 $m^3 m^{-3}$, 0.50, and -0.64, respectively. Calibration directly targeting ~~soil moisture~~soil-moisture reduced RMSE to 0.05 $m^3 m^{-3}$ and improved NSE to 0.12, while explaining approximately 50% of observed variability, Fig. 5. The multi-objective calibration produced similar RMSE

(0.05 m^3 m^{-3}) and R^2 (0.48), with improved alignment along the 1:1 line relative to the streamflow only model (Fig. 5; A2).

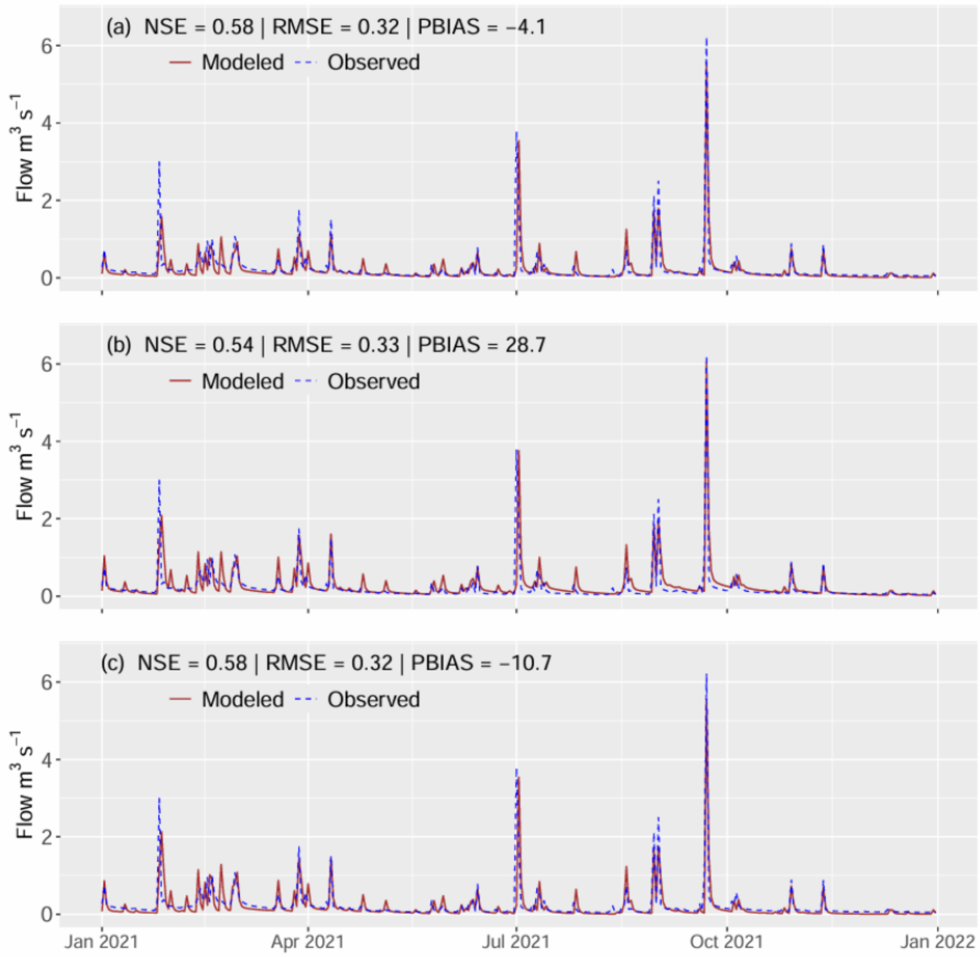

Figure 4: Model streamflow prediction performance calibration period a) streamflow only (SF) calibration b) ~~soil moisture~~soil-moisture only (DSM) calibration c) multi-objective (MO) calibration (see Fig. A3 for the ~~full~~complete time series).

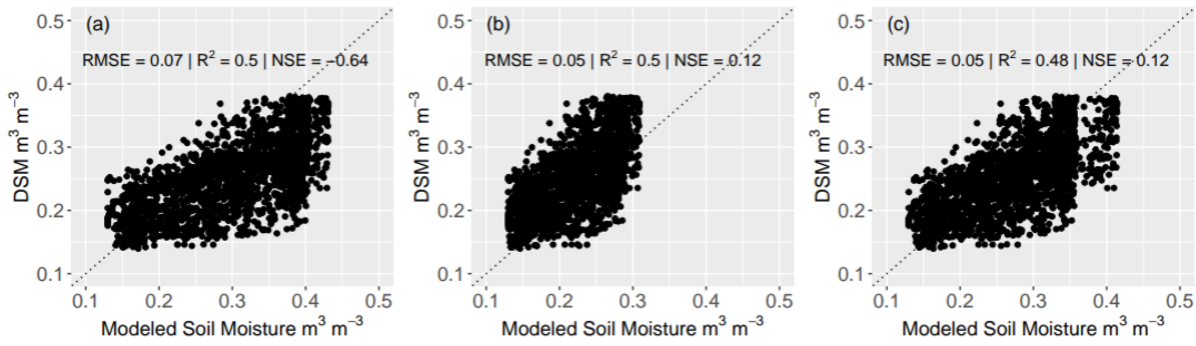

Figure 5: Model ~~soil moisture~~soil-moisture estimation performance during the calibration period compared against downscaled and bias corrected ~~soil moisture~~soil-moisture data calibrated on a) streamflow only (SF) calibration b) ~~soil moisture~~soil-moisture only (DSM) calibration c) multi-objective (MO) calibration.

3.3.2 Field-~~S~~scale ~~Soil Moisture~~Soil-Moisture-In-~~S~~situ Evaluation

Independent ~~field scale~~field-scale evaluation using in-situ soil- moisture measurements (0–120 mm) showed improved model performance when ~~soil moisture~~soil-moisture was included in the calibration. The streamflow calibrated model explained 50% of the observed ~~soil moisture~~soil-moisture variability ($R^2 = 0.5$), whereas the ~~soil moisture~~soil-moisture and multi-objective calibrations explained 88% of the observed ~~soil moisture~~soil-moisture variability ($R^2 = 0.88$) (Fig. 6). The multi-objective calibrated model reduced RMSE from 0.05 $m^3\ m^{-3}$ in the streamflow calibration to 0.03 $m^3\ m^{-3}$ and reduced PBIAS to −0.8%. Time-series comparison indicates reduced bias across a broader range of ~~soil moisture~~soil-moisture conditions for the multi-objective calibration approach (Fig. 7).

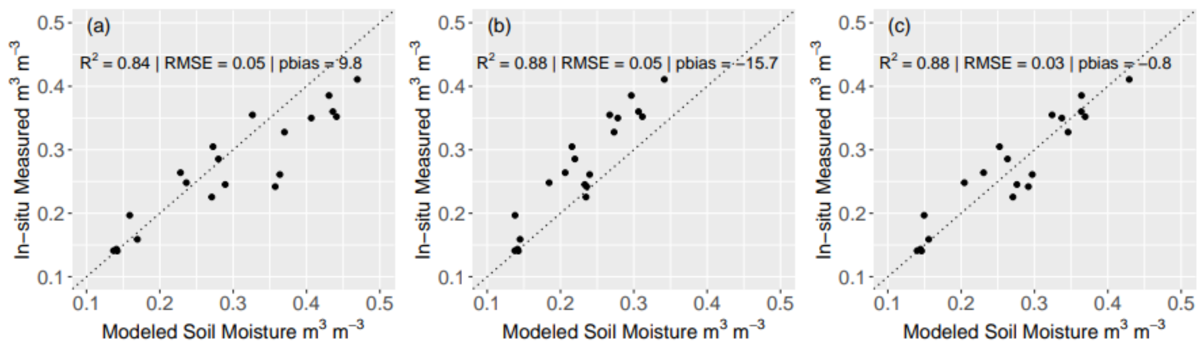

Figure 6: ~~Soil moisture~~Soil-moisture estimation performance of the three models in the evaluation period at ~~field scale~~field-scale against ~~field scale~~field-scale average ~~soil moisture~~soil-moisture estimate from in-situ measurements; a) streamflow only (SF) calibration b) ~~soil moisture~~soil-moisture only (DSM) calibration c) multi-objective (MO) calibration.

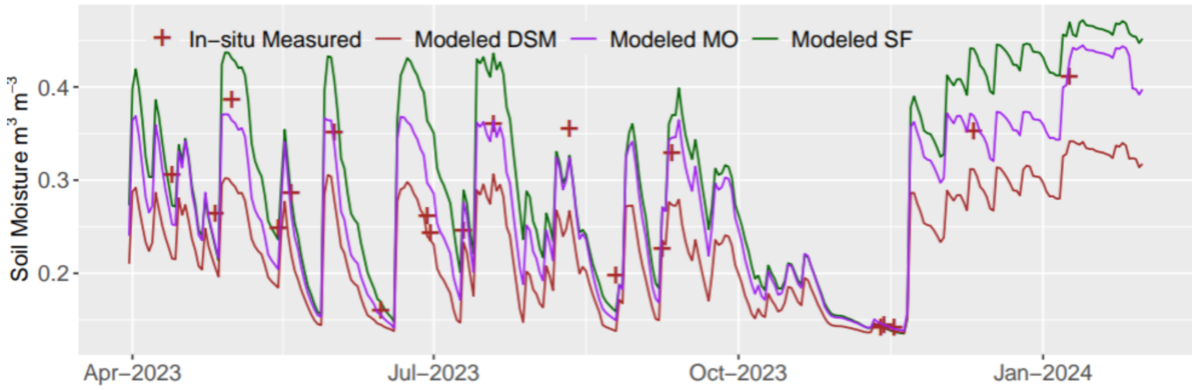

Figure 7: Temporal variability of modeled and measured ~~soil moisture~~soil-moisture for the three calibration approaches average over the top 120 mm soil layer; streamflow only (SF), ~~soil moisture~~soil-moisture only (DSM), and Multi-objective (MO).

3.4 Water Balance and Parameter Behavior

This section examines whether improvements in model performance metrics correspond to physically realistic hydrologic behavior or arise primarily from compensatory parameter adjustments. Surface runoff fractions were similar across models, reflecting comparable calibrated CN2 values. The average CN2 values were 42, 41.4, and 46.7 for the streamflow, multi-objective and ~~soil moisture~~soil-moisture calibrated models, respectively (Table 1), resulting in surface runoff values between 19.3% and 23.7% of the water balance (Fig. 8). The ~~soil moisture~~soil-moisture calibrated model produced lower ET and higher total streamflow relative to the other two approaches, whereas the streamflow and multi-objective calibrated models yielded similar partitioning among ET, lateral flow, and surface runoff components (Fig. 8).

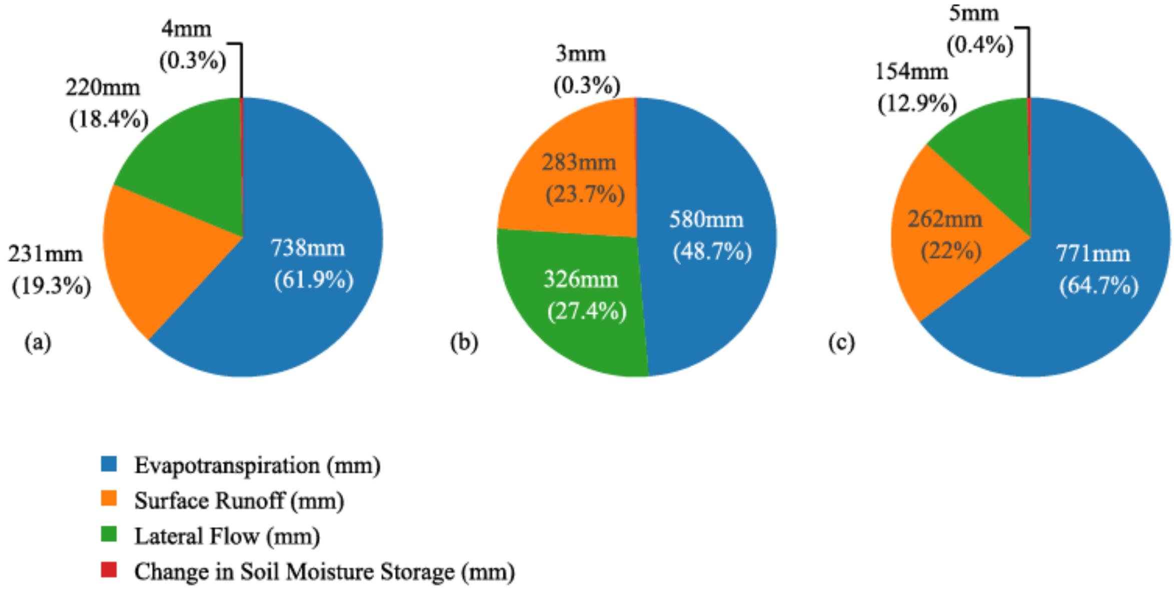

Figure 8: Model water balance estimation a) streamflow only (SF) calibration b) ~~soil moisture~~soil-moisture only (DSM) calibration c) multi-objective (MO) calibration.

The difference in ET and lateral flow components between the ~~soil moisture~~soil-moisture only calibrated model and the other two calibration approaches may be due to the reduced ~~soil moisture~~soil-moisture variability and reduced AWC in the ~~soil moisture~~soil-moisture only calibration. This calibration produces a lower mean and coefficient of variation (CV), compared to the other approaches (Table 2). While the values were comparable to the measured ~~soil moisture~~soil-moisture data, they diverged from the higher mean and variability simulated by the streamflow- and multi-objective calibrated models. When calibrating on streamflow, the optimization algorithm permits greater variability in ~~soil moisture~~soil-moisture related parameters because streamflow exhibits higher temporal variability (CV) than ~~soil moisture~~soil-moisture. In contrast, calibration against ~~soil moisture~~soil-moisture directly minimizes errors in the ~~soil moisture~~soil-moisture time series, constraining parameter variability, and favoring parameter sets that reproduce the lower variance structure of the ~~soil~~

~~moisture~~soil-moisture observations. As a result, the soil-moisture-only calibration converges on lower AWC and dampened ~~soil moisture~~soil-moisture dynamics, with corresponding implications for ET and lateral flow partitioning.

Table 2: ~~Soil moisture~~Soil-moisture variability during the calibration period (observed and modeled).

~~Soil Moisture~~Soil-moisture	**Mean ($cm^3\ cm^{-3}$)**	**Standard Deviation ($cm^3\ cm^{-3}$)**	**Coefficient of Variation (%)**
~~Soil moisture~~Soil-moisture data (measured)	0.26	0.06	22.4
From streamflow model	0.31	0.08	26.9
From ~~soil moisture~~soil-moisture model	0.23	0.05	21.8
From multi-objective model	0.28	0.07	24.8

3.5 Model Evaluation and Comparison

During the model evaluation period (01 Jan 2022 – 31 May 2024) all three models produced ~~comparative~~ comparable streamflow estimation performance with NSE values ranging from 0.55 to 0.56 and RMSE 0.25 $m^3\ m^{-\cancel{s}3}$ (Fig. 9). The ~~soil moisture~~soil-moisture-calibrated model exhibited positive bias in daily streamflow estimation (18.6%), primarily during low flow conditions. In contrast, the streamflow and multi-objective calibrated models showed an under-estimation bias of -11.9 and -21.7%, respectively (Fig. 9).

Overall, streamflow performance during the evaluation period was consistent with relative differences observed during calibration, confirming comparable predictive skill across calibration strategies under independent conditions.

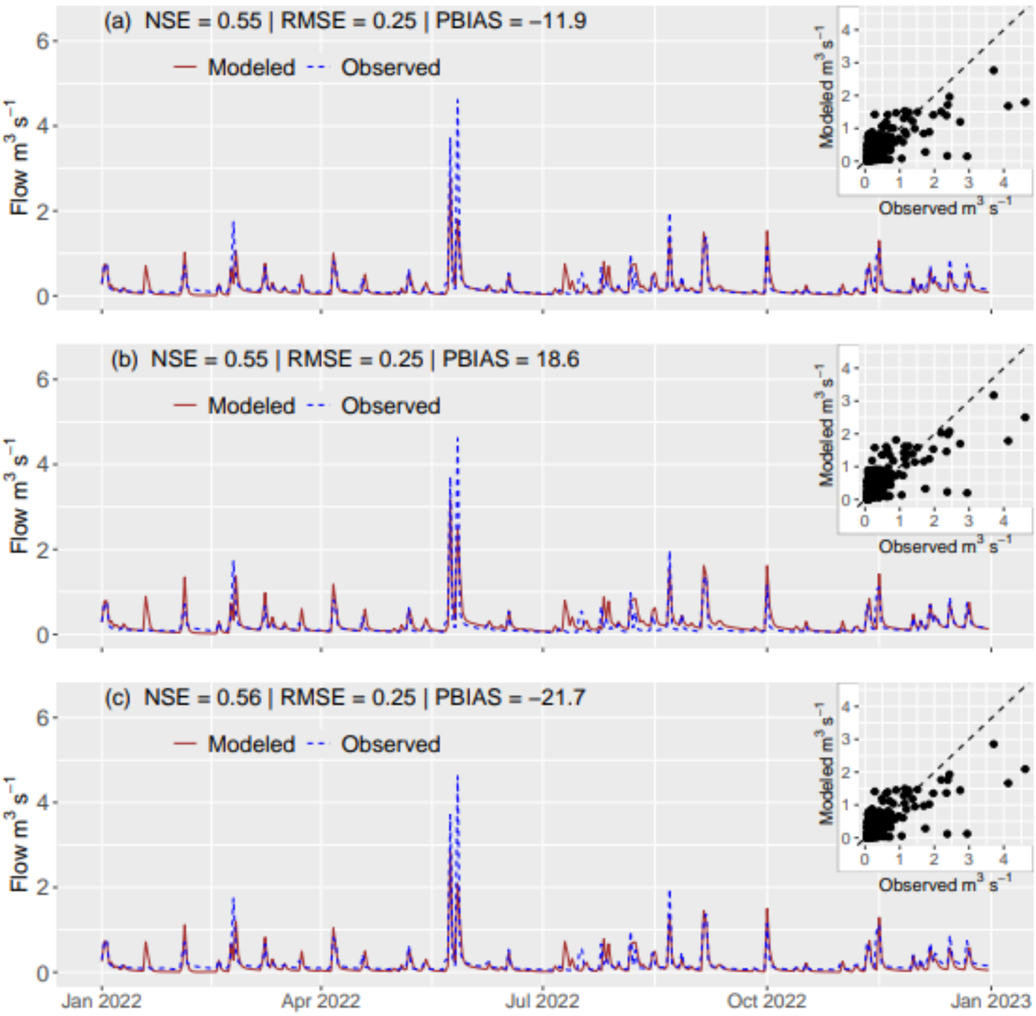

Figure 9: Model streamflow estimation performance evaluation period a) streamflow only (SF) calibration b) ~~soil moisture~~soil-moisture only (DSM) calibration c) multi-objective (MO) calibration (see also Fig. A4).

4 DISCUSSION

4.1 Effect of Downscaling and ~~Bias Correction~~Bias-Correction on the Soil-Moisture Signal

The downscaled satellite ~~soil moisture~~soil-moisture product captured the broad temporal patterns of wetting and drying at the ~~watershed scale~~watershed-scale but exhibited a reduced dynamic range and attenuated peak wetness relative to in-situ observations. This behavior is consistent with previous evaluations of satellite and downscaled ~~soil moisture~~soil-moisture products, which often reproduce large-scale temporal variability but smooth event and fine-scale extremes, particularly in topographically complex catchments (Brocca et al., 2017; Duethmann et al., 2022).

The ~~event based~~event-based ~~bias correction~~bias-correction~~ approach applied here~~ selectively enhanced ~~soil moisture~~soil-moisture responses during precipitation events while preserving dry period behavior and long-term seasonal structure. By conditioning the adjustment on effective precipitation, the correction addressed the commonly reported attenuation of peak wetness in pretrained downscaling products without altering the lower envelope of the ~~soil moisture~~soil-moisture signal (Duethmann et al., 2022; Xu et al., 2025). Importantly, the correction parameters were not derived from in-situ soil-moisture measurements, ensuring that the adjusted product remained independent of the evaluation data. The experimental design was intended to evaluate the utility of the final downscaled and bias-corrected soil-moisture product for calibration and was not designed to isolate the relative contributions of the native satellite retrieval, downscaling procedure, and bias-correction method. Consequently, the reported performance improvements should be interpreted as the combined effect of the preprocessing and calibration framework.

4.2 Impact of Calibration Strategy on Streamflow ~~Soil Moisture~~Soil-moisture Dynamics

Across calibration strategies, streamflow estimation performance remained broadly comparable, indicating that inclusion of satellite ~~soil moisture~~soil-moisture did not substantially degrade streamflow skill. This contrasts with studies reporting pronounced reductions in streamflow performance when models are calibrated solely on ~~soil moisture~~soil-moisture remote sensing products (Dangol et al., 2023; Kofidou & Gemitzi, 2023) or under certain multi-objective calibration frameworks (Duethmann et al., 2022; Mei et al., 2023). The results here ~~suggests~~suggest that the combination of the SWAT-VSA model structure and bias corrected satellite ~~soil moisture~~soil-moisture calibration target helped limit

~~trade-offs~~tradeoffs between contrasting internal ~~soil moisture~~soil-moisture state and preserving integrated streamflow fluxes.

Nevertheless, the calibration strategy influenced bias patterns. The ~~soil moisture~~soil-moisture only calibrated model consistently overestimated low flows, whereas the streamflow- and multi-objective calibrated models exhibited underestimation bias (Fig. A1). Duethmann et al. (2022) showed that streamflow underestimation was more pronounced when ~~soil moisture~~soil-moisture was included in the calibration. Such differences among calibration strategies may not be simple parameter trade-off issue but rather could be related to model structure, for instance potential deficiencies in the evapotranspiration mechanism (Rajib et al. 2016), potentially leading to inadequate handling of water balance partitioning and over-compensation of related parameters.

In contrast, ~~soil moisture~~soil-moisture estimation, particularly at the ~~field scale~~field-scale, was more sensitive to calibration strategy. Both ~~soil moisture~~soil-moisture only and multi-objective calibration improved agreement with observed soil-moisture dynamics relative to streamflow-only calibration, consistent with studies demonstrating the value of soil-moisture data for constraining internal model states (Rajib & Merwade, 2016; Mei et al., 2023).

The calibration strategies yielded satisfactory streamflow performance (NSE = 0.54-0.58). Although increased levels of streamflow skill (NSE = 0.6) have been reported for this same study watershed using SWAT (e.g., Thilakarathne et al., 2018), direct comparison of NSE values could be misleading as streamflow performance here was achieved over a long calibration period (~10 years) encompassing substantial hydrologic variability. This indicates that the calibrated parameter set maintains reasonable process behavior across a broad range of flow regimes and antecedent moisture conditions, rather than being tuned to short-term or event specific dynamics.

Parameters describing soil physical properties, including bulk density, available water capacity, and saturated hydraulic conductivity, deviated from baseline values in the soil database by −7%, +155%, and +136%, respectively. Such adjustments are consistent with previous findings showing that regional or large-scale soil datasets often fail to represent local soil characteristics, including texture, horizon thickness, and organic matter content (Buell, 2022; Fuka et al., 2016). Accordingly, allowing substantial flexibility in soil property parameters during calibration is justified for improving hydrologic performance in small, topographically complex watersheds.

4.3 Statistical Improvements versu~~e~~s Hydrologic Realism

Although ~~soil moisture~~soil-moisture only calibration produced measurable improvements in statistical agreement with ~~soil moisture~~soil-moisture observations, these gains did not uniformly translate into improved behavior across all hydrologic processes. The ~~soil moisture~~soil-moisture calibrated model better reproduced soil surface wetting dynamics but exhibited biased low flow behavior and altered water-balance partitioning. This pattern illustrates a central concern raised in recent multi-objective calibration studies: improvements in fit to a particular variable may reflect parameter compensation rather than improved process representation (Gupta et al., 2009; Duethmann et al., 2022; Mei et al., 2023).

The multi-objective calibration provided more balanced results by simultaneously constraining streamflow and ~~soil moisture~~soil-moisture responses. Independent ~~field scale~~field-scale evaluation showed that this approach reduced both RMSE and bias across a wider range of ~~soil moisture~~soil-moisture conditions while preserving streamflow performance comparable to streamflow only calibration. These findings align with previous work showing that multi-objective approaches can reduce equifinality and improve internal consistency, even if individual hydrologic performance metrics do not increase dramatically (Rajib et al., 2016; Silvestro et al., 2015).

Crucially, this study reinforces the distinction between improved statistical fit and improved hydrologic realism. Gains in ~~soil moisture~~soil-moisture metrics alone should not be interpreted as evidence of improved system representation unless supported by independent evaluation and water balance diagnostics.

4.4 Parameter Behavior, Compensation, and Structural Model Constraints

Calibrated curve number (CN2) values distributed across topographic index (TI) classes reveal strongly heterogeneous runoff contributions consistent with saturation excess hydrology. TI class 1, which covers 56% of the watershed, contributes only ~9% of total surface runoff on a per area basis, while TI class 3, representing just 6% of the watershed, generates approximately 30%. Such disproportional contributions are characteristic of saturation excess systems, where runoff is concentrated in low lying, convergent landscape positions receiving sustained subsurface moisture inputs from upslope areas (Dahlke et al., 2009; Easton et al., 2008; Lyon et al., 2004). In SWAT-VSA, this behavior is indirectly represented by redistributing CN2 values according to local storage deficit, linking runoff generation to ~~terrain controlled~~terrain-controlled wetness patterns.

The surface runoff lag coefficient (SURLAG) was higher in the streamflow only calibration than in the other approaches; however, this had a negligible impact on runoff timing because the watershed time of concentration is less than 1.5 hr. Differences among calibration strategies were more pronounced for evapotranspiration related parameters. The multi-objective calibration favored ESCO and EPCO values that increased water extraction from deeper soil layers, resulting in higher ET and reduced excess runoff. In contrast, the ~~soil moisture~~soil-moisture only calibration produced ESCO and EPCO values near unity that effectively compensated for one another, dampening vertical moisture redistribution and contributing to reduced ET.

Groundwater and baseflow parameters had little influence across all calibrations, with near zero percolation estimated, consistent with shallow soils and limited vertical drainage in saturation excess landscapes. Differences in calibrated parameter values highlight compensatory behavior: ~~soil moisture~~soil-moisture only calibration favored lower available water content (AWC) and ET, increasing simulated streamflow while improving surface ~~soil moisture~~soil-moisture fit but altering internal water balance partitioning.

These outcomes reflect structural constraints within SWAT-VSA and SWAT more broadly, which represent unsaturated flow using vertically lumped soil layers and do not explicitly simulate lateral redistribution of ~~soil moisture~~soil-moisture among HRUs (Rajib et al., 2016). In saturation excess systems, where downslope redistribution and hydrologic connectivity dominate wetness evolution, these simplifications limit the model's ability to translate improved surface ~~soil moisture~~soil-moisture fit into realistic subsurface fluxes and recession behavior (Easton et al., 2008; Lyon et al., 2004).

Multi-objective calibration mitigated these limitations by jointly constraining streamflow and ~~soil moisture~~soil-moisture, reducing extreme parameter combinations and dampening compensation effects. When combined with physically informed preprocessing, ~~soil moisture~~soil-moisture observations can complement streamflow data by constraining antecedent moisture conditions that govern runoff generation (Brocca et al., 2017; Wagner et al., 2007). Here, the ~~event based~~event-based ~~bias correction~~bias-correction approach likely improved the hydrologic relevance of the satellite ~~soil moisture~~soil-moisture signal, contributing to improved consistency in both ~~soil moisture~~soil-moisture and streamflow simulation (Bekele & Nicklow, 2007; Rajib et al., 2016).

4.5 Parameter Uncertainty and Equifinality

While the previous section focused on how different calibration strategies alter parameter values and process behavior, this section examines how those strategies affect parameter uncertainty and equifinality.

Consistent with previous studies (Rajib & Merwade, 2016; Silvestro et al., 2015), parameter uncertainty was lowest under multi-objective calibration (Fig. 10), particularly for soil-water- and evapotranspiration-related parameters. Figure 10 shows that the range of acceptable values for AWC, Ksat, ESCO, and EPCO was substantially narrower under multi-objective calibration than under either streamflow-only or soil-moisture-only calibration. This reduced parameter spread indicates fewer equally acceptable parameter combinations and therefore reduced equifinality (Beven, 1993). By simultaneously constraining streamflow and soil-moisture dynamics, the multi-objective calibration more effectively restricted the feasible parameter space and improved confidence in parameters governing soil-water storage and vertical moisture redistribution. Together with the water-balance analysis, these results suggest that multi-objective calibration not only improved model performance but also reduced compensatory parameter behavior.

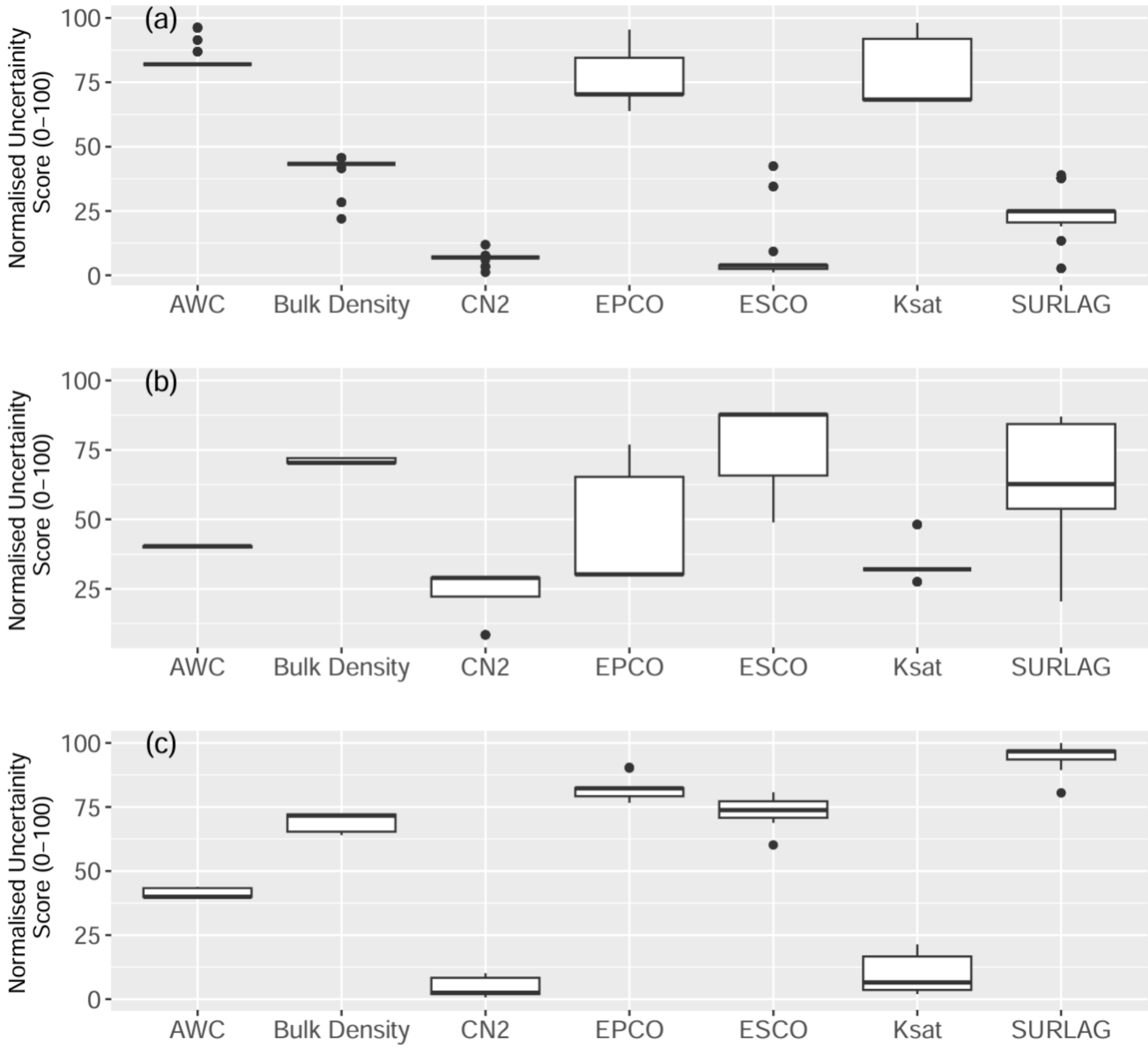

Figure 10: Parameter uncertainty estimate derived from DEoptim calibration iterations for a) streamflow only, b) ~~soil moisture~~soil-moisture only and, c) multi-objective calibration. The height of the boxplot demonstrates the range of different values the parameters took while yielding acceptable model performance. The values are calculated using the normalized uncertainty score from Kumar & Merwade (2009), where 0 and 100 represent the minimum and maximum parameter value as defined by the normalized calibration range.

4.6 Implications for Small Saturation-Excess Watersheds

The results demonstrate that downscaled, empirically bias corrected satellite ~~soil moisture~~soil-moisture data can improve internal hydrologic state estimation in small, saturation excess dominated watersheds when combined with a terrain-informed model structure. The SWAT-VSA framework, using TI based HRUs and TI-weighted field-scale evaluation, enables direct assessment of whether calibration improvements extend to management relevant scales (Easton et al., 2008; Asfaw et al., 2025).

At the same time, the findings underscore the need for caution. ~~Soil moisture~~Soil-moisture only calibration can yield misleading improvements if evaluated solely on statistical metrics, particularly in models with simplified representations of unsaturated and lateral ~~soil moisture~~soil-moisture processes. Multi-objective calibration offers a more robust balance between surface wetness dynamics and integrated flow behavior, although its effectiveness remains dependent on watershed characteristics and model structure (Duethmann et al., 2022; Mei et al., 2023). While the added complexity of downscaling and multi-objective calibration is warranted in this small, saturation excess watershed, caution is needed in generalizing these findings to other settings or assuming that improved satellite ~~soil moisture~~soil-moisture fit automatically implies improved hydrologic realism.

4.7 Limitations

This study was conducted in a small (14.5 km²), saturation excess dominated watershed. While appropriate for evaluating ~~soil moisture~~soil-moisture driven calibration in terrain controlled hydrologic systems, this limits the generalizability of the findings. In larger or more heterogeneous watersheds, greater spatial variability in precipitation, land use, soils, and hydrologic connectivity may influence both the downscaled ~~soil moisture~~soil-moisture behavior and the calibration performance. In particular, the ~~event based~~event-based ~~bias correction~~bias-correction approach applied here relies on watershed average effective precipitation and may not capture spatially variable wetting responses in more complex basins.

The applicability of the SWAT-VSA model is restricted to saturation excess runoff environments, where shallow soil storage deficits and topographic convergence largely control runoff generation. Watersheds dominated by infiltration excess processes, weak terrain control, or arid and semi-arid conditions may not benefit from the TI-based structure. Nonetheless, saturation excess processes are widespread in humid temperate regions of the United States (Buchanan et al., 2018) as well as globally, suggesting that this approach remains relevant to a broad class of headwater catchments.

The downscaled ~~soil moisture~~soil-moisture product underestimates peak wetness during high moisture periods. Although the ~~bias correction~~bias-correction improves event scale responsiveness while preserving long-term temporal structure, it does not resolve underlying spatial or physical limitations of the satellite product. Consequently, the performance improvements should be interpreted as enhanced temporal constraint rather than complete correction of soil-moisture uncertainty. Furthermore, the relative contributions of the Enhanced SMAP product, machine-learning downscaling, and event-based bias-correction were not evaluated independently. Future work should compare calibration performance across these intermediate products to better quantify their individual contributions.

Overall, the findings should be interpreted within these constraints. Application of this framework beyond small, saturation excess watersheds will require careful consideration of watershed characteristics and evaluation across additional sites before broader inferences are made.

5 CONCLUSIONS

This study evaluated the utility of downscaled satellite ~~soil moisture~~soil-moisture data for calibrating a SWAT-VSA model in a small watershed for enhanced estimation of ~~field scale~~field-scale ~~soil moisture~~soil-moisture variability. The results show that leveraging downscaled satellite ~~soil moisture~~soil-moisture data substantially improves estimation of temporal variability of ~~soil moisture~~soil-moisture without deteriorating the model accuracy in streamflow estimation. Multi-objective calibration using both streamflow and ~~soil moisture~~soil-moisture data ~~outperformed single-objective approaches by improving estimation of both variables while reducing parameter uncertainty~~ improved soil-moisture performance and maintained streamflow performance comparable to streamflow-only calibration. Calibration based solely on ~~soil moisture~~soil-moisture led to improved ~~soil moisture~~soil-moisture performance with minimal declines in streamflow skill relative to streamflow only calibration.

Machine learning based satellite ~~soil moisture~~soil-moisture downscaling, using the 'mlrhsm' package in R, provided ~~soil moisture~~soil-moisture data of sufficient resolution and temporal fidelity to calibrate a high-resolution SWAT-VSA model in ~~a small~~this watershed. Parameter uncertainty varied with calibration approach; soil parameters were better constrained with ~~soil moisture~~soil-moisture data, and streamflow parameters with streamflow data. Multi-objective calibration reduced parameter uncertainty. Long-term water balance estimates varied widely across the three calibration approaches, indicating the need for further evaluation, particularly using independent evapotranspiration measurements, to assess how ~~soil moisture~~soil-moisture constraints influence internal flux partitioning.

Overall, these findings highlight the potential of remotely sensed ~~soil moisture~~soil-moisture products to improve hydrologic model calibration, particularly in data-~~-~~limited and ungauged basins.

However, further evaluation is required in ungauged watersheds where no local ~~soil moisture~~soil-moisture or streamflow data are available for validation or qualitative assessment. Given their global coverage, satellite ~~soil moisture~~soil-moisture datasets offer a promising pathway for enhancing both streamflow and ~~soil moisture~~soil-moisture estimation when combined with terrain informed model structures and multi-objective calibration frameworks.

APPENDIX

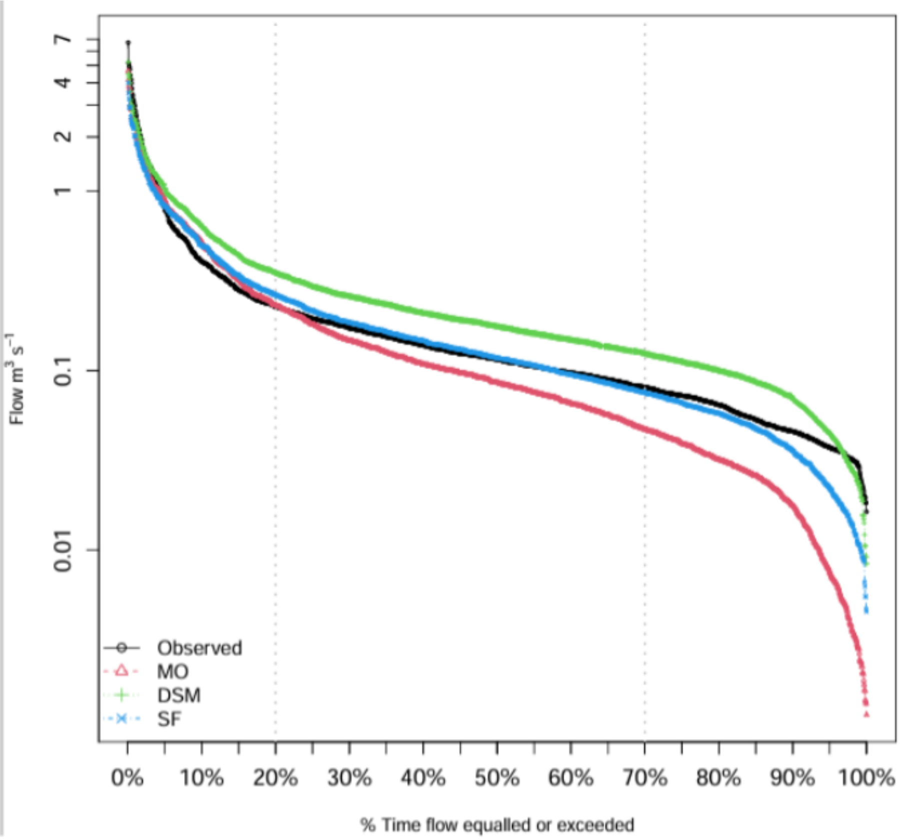

Figure A1: Flow duration curves comparing observed daily streamflow with simulations from the ~~soil moisture~~soil-moisture only (DSM), streamflow only (SF), and multi-objective (MO) calibration strategies. Differences among curves illustrate how calibration targets influence hydrologic realism: DSM captures surface wetting dynamics, but underestimates recession flows and high-flow peaks, whereas MO and SF better reproduce the observed distribution across both high-frequency (low flows) and low-frequency (peak flow) events.

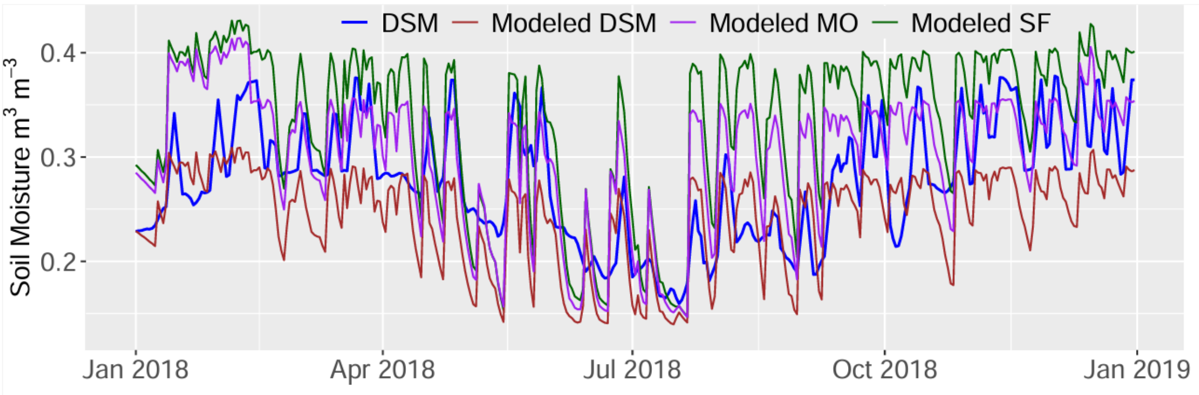

Fig. A2: Time series of modeled surface ~~soil moisture~~soil-moisture (50 mm) from the three calibration approaches and DSM data; calibrated on DSM data (Modeled DSM), Multi-objective calibration using DSM data and streamflow (Modeled MO), calibrated on streamflow (Modeled SF).

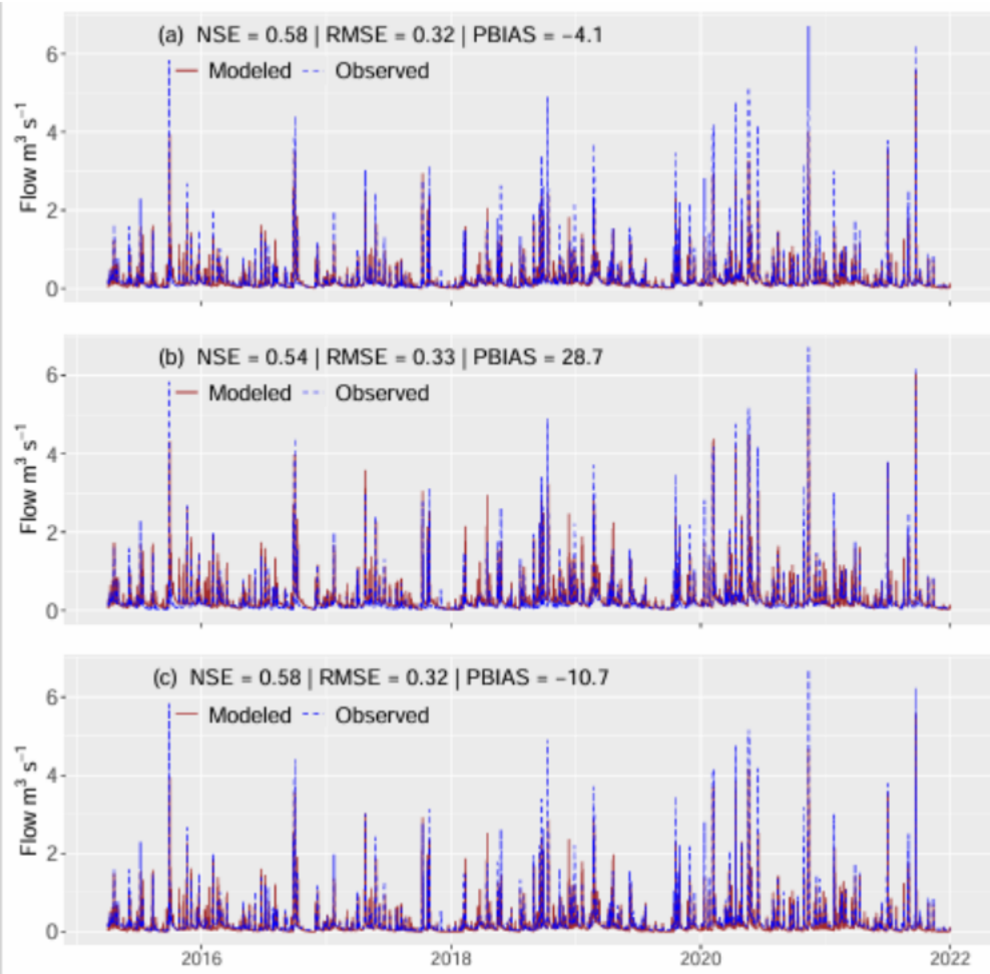

Figure~~.~~ A3: Full time series of model streamflow prediction performance calibration period a) streamflow only (SF) calibration b) ~~soil moisture~~soil-moisture only (DSM) calibration c) multi-objective (MO) calibration.

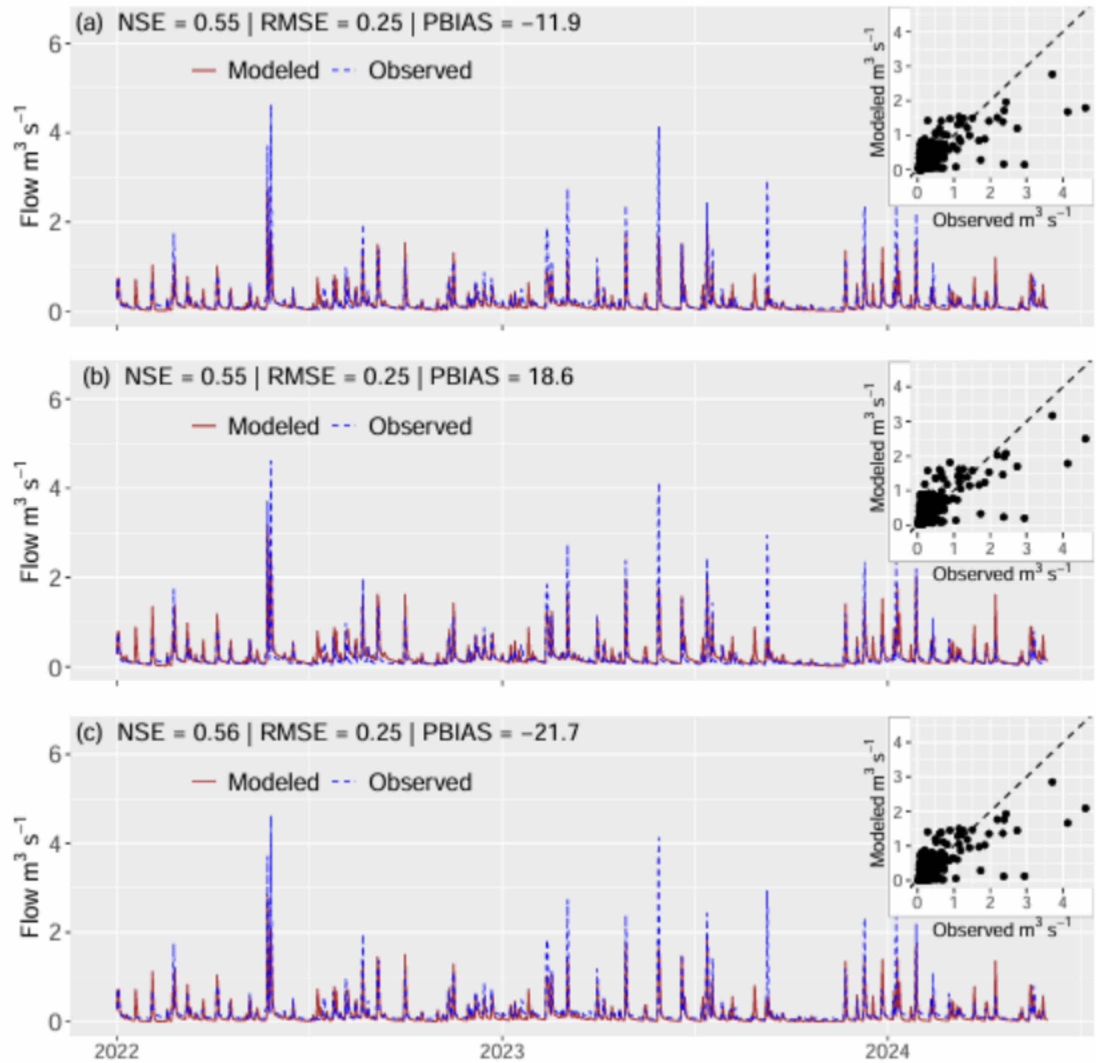

Figure A4: Model streamflow prediction performance evaluation period a) streamflow only (SF) calibration b) ~~soil moisture~~soil-moisture only (DSM) calibration c) multi-objective (MO) calibration.

Table A1. ~~Soil moisture~~Soil-moisture data preprocessing and model integration

Source	Nominal / effective depth represented	How we aggregate to watershed/field	Model layer used for comparison	Role in this study
Downscaled satellite SM (mlhrsm from Enhanced SMAP)	Surface layer (0–50 mm)	Average all 500 m pixels intersecting the watershed to a daily watershed mean	0–50 mm SWAT layer	Calibration target in DSM and MO scenarios
SWAT-VSA model output	Discrete layers: 0–50 mm and 50–120 mm (plus standard deeper layers)	HRU outputs aggregated to watershed or field boundaries using TI-class/HRU area weights	0–50 mm (for satellite comparison); 0–50 mm + 50–120 mm composite = 0–120 mm (for field comparison)	Calibration (0–50 mm) and Evaluation (0–120 mm)
In-situ TDR measurements (25 points)	0–120 mm (field sampling depth)	TI-class-weighted average across the 4.2 ha pasture to obtain a field-scale mean	0–120 mm model composite	Independent ~~evaluation~~of model calibration, but used in Pareto solution selection~~ only~~

Note: The 0–50 mm equivalent designation for the satellite product is an operational alignment for comparability; it does not imply that the satellite directly senses 50 mm uniformly. The purpose is to avoid mismatched depths during calibration and to keep field-scale evaluation at the measured 0–120 mm depth.

CODE AVAILABILITY

Available upon request

DATA AVAILABILITY

The majority of the data used in this study is publicly available.

TEAM LIST

Binyam Workeye Asfaw; Siam Maksud; Daniel R. Fuka; Amy S. Collick; Robin R. White; Zachary M. Easton

AUTHOR CONTRIBUTION

Binyam Workeye Asfaw: Conceptualization; data curation; formal analysis; investigation; methodology; visualization; writing—original draft; writing—review and editing.

Siam Maksud: Data curation; writing—review and editing.

Daniel R. Fuka: Conceptualization; methodology; writing—review and editing.

Amy S. Collick: Methodology; writing-review and editing

Robin R. White: Conceptualization; funding acquisition; project administration.

Zachary M. Easton: Conceptualization; data curation; formal analysis; funding acquisition; project administration; writing—original draft; writing—review and editing.

COMPETING INTERESTS

Authors declare that they have no competing interest.

ACKNOWLEDGEMENTS

We acknowledge USDA CPS program for the financial support.

FINANCIAL SUPPORT

This research was funded by USDA CPS award number 2021-67021-34769.

REFERENCES

Abbaszadeh, P., Moradkhani, H., Gavahi, K., Kumar, S., Hain, C., Zhan, X., Duan, Q., Peters-Lidard, C., & Karimiziarani, S. (2021). High-resolution SMAP satellite soil moisture product: Exploring the opportunities. *Bulletin of the American Meteorological Society*, *102*(4), 309–315.

Arnold, J. G., Moriasi, D. N., Gassman, P. W., Abbaspour, K. C., White, M. J., Srinivasan, R., Santhi, C., Harmel, R. D., Van Griensven, A., & Van Liew, M. W. (2012). SWAT: Model use, calibration, and validation. *Transactions of the ASABE*, *55*(4), 1491–1508.

Asfaw, B. W., Fuka, D. R., Collick, A. S., White, R. R., & Easton, Z. M. (2025). Characterizing the topographic index as a tool to represent spatial soil moisture: The effect of classification approach, digital elevation model type, and resolution. *Vadose Zone Journal*, *24*(4), e70031. https://doi.org/10.1002/vzj2.70031

Azimi, S., Dariane, A. B., Modanesi, S., Bauer-Marschallinger, B., Bindlish, R., Wagner, W., & Massari, C. (2020). Assimilation of Sentinel 1 and SMAP – based satellite soil moisture retrievals into SWAT hydrological model: The impact of satellite revisit time and product spatial resolution on flood simulations in small basins. *Journal of Hydrology*, *581*. https://doi.org/10.1016/j.jhydrol.2019.124367

Bekele, E. G., & Nicklow, J. W. (2007). Multi-objective automatic calibration of SWAT using NSGA-II. *Journal of Hydrology*, *341*(3), 165–176. https://doi.org/10.1016/j.jhydrol.2007.05.014

Beven, K. (1993). Prophecy, reality and uncertainty in distributed hydrological modelling. *Advances in Water Resources*, *16*(1), 41-51. https://doi.org/10.1016/0309-1708(93)90028-E

Beven, K. J., Kirkby, M. J., Freer, J. E., & Lamb, R. (2021). A history of TOPMODEL. *Hydrology and Earth System Sciences*, *25*(2), 527–549. https://doi.org/10.5194/hess-25-527-2021.

Blank, J., & Deb, K. (2020). Pymoo: Multi-Objective Optimization in Python. *IEEE Access*, *8*, 89497–89509. IEEE Access. https://doi.org/10.1109/ACCESS.2020.2990567

Bocinsky, R. K., Beaudette, D., Chamberlain, S., Hollister, J., & Gustavsen, J. (2025). *FedData: Download Geospatial Data Available from Several Federated Data Sources* (Version 4.3.0). https://cran.r-project.org/web/packages/FedData/index.html

Brocca, L., Ciabatta, L., Massari, C., Camici, S., & Tarpanelli, A. (2017). Soil m~~M~~oisture for h~~H~~ydrological a~~A~~pplications: Open q~~Q~~uestions and n~~N~~ew o~~O~~pportunities. *Water*, *9*(2), 2. https://doi.org/10.3390/w9020140

Brocca, L., Melone, F., Moramarco, T., & Morbidelli, R. (2010). Spatial-temporal variability of soil moisture and its estimation across scales. *Water Resources Research*, *46*(2). https://doi.org/10.1029/2009WR008016

Buell, E. N. (2022). *Improved environmental characterization to support natural resource decision making: (1) Distributed soil characterization, and (2) T~~t~~reatment of l~~L~~egacy n~~N~~utrients*. http://hdl.handle.net/10919/112013

Buchanan, B., D.A. Auerbach, J. Knighton, D. Evensen, D. R. Fuka Z.M. Easton, M. Wieczorek, J.A. Archibald, B. McWilliams, M.T. Walter . 2018. Estimating dominant runoff modes across the conterminous United States. Hydrological Processes. https://doi.org/10.1002/hyp.13296

Chan, S. K., Bindlish, R., O'Neill, P., Jackson, T., Njoku, E., Dunbar, S., Chaubell, J., Piepmeier, J., Yueh, S., Entekhabi, D., Colliander, A., Chen, F., Cosh, M. H., Caldwell, T., Walker, J., Berg, A., McNairn, H., Thibeault, M., Martínez-Fernández, J., Uldall, F., Seyfried, M., Bosch, D., Starks, P., Holifield Collins, C., Prueger, J., Van Der Velde, R., Asanuma, J., Palecki, M., Small, E. E., Zreda, M., Calvet, J., Crow, W. T., & Kerr, Y. (2018). Development and assessment of the SMAP enhanced passive soil moisture product. *Remote Sensing of Environment*, *204*, 931–941. https://doi.org/10.1016/j.rse.2017.08.025

Cho, E., Moon, H., & Choi, M. (2015). First a~~A~~ssessment of the Advanced Microwave Scanning Radiometer 2 (AMSR2) a~~S~~oil m~~M~~oisture c~~C~~ontents in Northeast Asia. *Journal of Meteorology. Series 2*, *93*(1), 117–129. https://doi.org/10.2151/jmsj.2015-008

Colliander, A., T.J. Jackson, R. Bindlish, S. Chan, N. Das, S.B. Kim, M.H. Cosh, R.S. Dunbar, L. Dang, L. Pashaian, J. Asanuma, K. Aida, A. Berg, T. Rowlandson, D. Bosch, T. Caldwell, K. Caylor, D. Goodrich, H. al Jassar, E. Lopez-Baeza, J. Martínez-Fernández, A. González-Zamora, S. Livingston, H. McNairn, A. Pacheco, M. Moghaddam, C. Montzka, C. Notarnicola, G. Niedrist, T. Pellarin, J. Prueger, J. Pulliainen, K. Rautiainen, J. Ramos, M. Seyfried, P. Starks, Z. Su, Y. Zeng, R. van der Velde, M. Thibeault, W. Dorigo, M. Vreugdenhil, J.P. Walker, X. Wu, A. Monerris, P.E. O'Neill, D. Entekhabi, E.G. Njoku, & S. Yueh. (2017). Validation of SMAP surface soil moisture products with core validation sites. *Remote Sensing of Environment*, *191*, 215–231. https://doi.org/10.1016/j.rse.2017.01.021

Dahlke, H. E., Easton, Z. M., Fuka, D. R., Lyon, S. W., & Steenhuis, T. S. (2009). Modelling variable source area dynamics in a CEAP watershed. *Ecohydrology*, *2*(3), 337–349. https://doi.org/10.1002/eco.58

Dangol, S., Zhang, X., Liang, X.-Z., Anderson, M., Crow, W., Lee, S., Moglen, G. E., & Mccarty, G. W. (2023). Multivariate c~~C~~alibration of the SWAT ~~M~~model using remotely sensed datasets. *Remote Sensing*, 2417 (22 pp.). https://doi.org/10.3390/rs15092417

Das, N. N., Entekhabi, D., Kim, S., Jagdhuber, T., Dunbar, S., Yueh, S., O’Neill, P. E., Colliander, A., Walker, J., & Jackson, T. J. (2018). High-resolution enhanced product based on SMAP active-passive approach using sentinel 1A and 1B SAR data. *International Archives of the Photogrammetry, Remote Sensing and Spatial Information Sciences. XLII–5*, 203–205. https://doi.org/10.5194/isprs-archives-XLII-5-203-2018

De Santis, D., Biondi, D., Crow, W. T., Camici, S., Modanesi, S., Brocca, L., & Massari, C. (2021). Assimilation of satellite soil moisture products for river flow prediction: An extensive experiment in over 700 catchments throughout ~~europe~~Europe. *Water Resources Research*, *57*(6). https://doi.org/10.1029/2021WR029643

Deb, K., Agrawal, S., Pratap, A., & Meyarivan, T. (2000). A f~~F~~ast e~~E~~litist n~~N~~on-dominated s~~S~~orting g~~G~~enetic a~~A~~lgorithm for m~~M~~ulti-objective o~~O~~ptimization: NSGA-II. In M. Schoenauer, K. Deb, G. Rudolph, X. Yao, E. Lutton, J. J. Merelo, & H.-P. Schwefel (Eds.), *Parallel Problem Solving from Nature PPSN VI* (pp. 849–858). Springer. https://doi.org/10.1007/3-540-45356-3_83

Duethmann, D., Smith, A., Soulsby, C., Kleine, L., Wagner, W., Hahn, S., & Tetzlaff, D. (2022). Evaluating satellite-derived soil moisture data for improving the internal consistency of process-based ecohydrological modelling. *Journal of Hydrology*, *614*, 128462. https://doi.org/10.1016/j.jhydrol.2022.128462

Easton, Z. M., Fuka, D. R., Walter, M. T., Cowan, D. M., Schneiderman, E. M., & Steenhuis, T. S. (2008). Re-conceptualizing the S~~s~~oil and W~~w~~ater A~~a~~ssessment T~~t~~ool (SWAT) model to predict runoff from variable source areas. *Journal of Hydrology*, *348*(3), 279–291. https://doi.org/10.1016/j.jhydrol.2007.10.008

Eini, M. R., Massari, C., & Piniewski, M. (2023). Satellite-based soil moisture enhances the reliability of agro-hydrological modeling in large transboundary river basins. *Science of The Total Environment*, *873*, 162396. https://doi.org/10.1016/j.scitotenv.2023.162396

Entekhabi, D., Reichle, R. H., Koster, R. D., & Crow, W. T. (2010). Performance metrics for soil moisture retrievals and application requirements. *Journal of Hydrometeorology*, https://doi.org/10.1175/2010JHM1223.1

~~Entekhabi, D., Yueh, Si., & De Lannoy, G. (2014). *SMAP handbook*.~~

Entekhabi, D., Yueh, S., and de Lannoy, G. (2014). SMAP Handbook, Jet Propulsion Laboratory, California Institute of Technology, Pasadena, CA, USA, 2014, available at: https://smap.jpl.nasa.gov/ (last access: July 2026).

~~Food and Agriculture Organization of the United Nations (FAO). (2007). *FAO digital soil map of the world (DSMW)*. https://www.fao.org/land-water/land/land-governance/land-resources-planning-toolbox/category/details/en/c/1026564/~~

Food and Agriculture Organization of the United Nations (FAO). (2007). FAO Digital Soil Map of the World (DSMW). FAO, Rome, Italy. https://www.fao.org/land-water/land/land-governance/land-resources-planning-toolbox/category/details/en/c/1026564/

Fuka, D. R., Collick, A. S., Kleinman, P. J. A., Auerbach, D. A., Harmel, R. D., & Easton, Z. M. (2016). Improving the spatial representation of soil properties and hydrology using topographically derived initialization processes in the SWAT model. *Hydrological Processes*. https://doi.org/10.1002/hyp.10899

Fuka, D. R., & Easton, Z. M. (2016). *TopoSWAT s~~S~~ource. Figshare. Dataset.* https://doi.org/10.6084/m9.figshare.1342823.v4.

Fuka, D. R., W, M., A, J., Garna, R. K., & Easton, Z. M. (2013). *EcoHydRology: A community modeling foundation for EcoHydrology* (Version R package version 0.4.19 [software]). https://CRAN.R-project.org/package=EcoHydRology

Garna, R. K., Easton, Z. M., Faulkner, J. W., Collick, A. S., & Fuka, D. R. (2023). Employing higher density lower reliability weather data from the Global Historical Climatology Network monitors to generate serially complete weather data for watershed modelling. *Hydrological Processes*, *37*(11), e15013. https://doi.org/10.1002/hyp.15013

Gupta, H. V., Kling, H., Yilmaz, K. K., & Martinez, G. F. (2009). Decomposition of the mean squared error and NSE performance criteria: Implications for improving hydrological modelling. *Journal of Hydrology, 377(1)*, 80–91. https://doi.org/10.1016/j.jhydrol.2009.08.003

H SAF. (2021). *ASCAT Surface Soil Moisture Climate Data Record v7 12.5 km sampling—Metop, EUMETSAT SAF on Support to Operational Hydrology and Water Management*. https://doi.org/10.15770/EUM_SAF_H_0009

~~Han, L., Wang, C., Liu, Q., Wang, G., Yu, T., Gu, X., & Zhang, Y. (2020). Soil Moisture Mapping Based on Multi-Source Fusion of Optical, Near-Infrared, Thermal Infrared, and Digital Elevation Model Data via the Bayesian Maximum Entropy Framework. *Remote Sensing*, *12*(23). https://doi.org/10.3390/rs12233916~~

Hofmeister, K. L., Cianfrani, C. M., & Hession, W. C. (2015). Complexities in the stream temperature regime of a small mixed-use watershed, Blacksburg, VA. *Ecological Engineering*, *78*, 101–111. https://doi.org/10.1016/j.ecoleng.2014.05.019

Jin, S., Dewitz, J., Danielson, P., Granneman, B., Costello, C., Smith, K., & Zhu, Z. (2023). National Land Cover Database 2019: A New strategy for creating clean leaf-on and leaf-off ~~landsat~~Landsat composite images. *Journal of Remote Sensing*, *3*, 0022. https://doi.org/10.34133/remotesensing.0022

Ketabchy, M. (2018). *Thermal evaluation of an urbanized watershed using SWMM and MINUHET: A case study of Stroubles Creek Watershed, Blacksburg, VA* [Thesis, Virginia Tech]. https://vtechworks.lib.vt.edu/handle/10919/81977

Kofidou, M., & Gemitzi, A. (2023). Assimilating s~~S~~oil moisture information to improve the performance of SWAT h~~H~~ydrological m~~M~~odel. *Hydrology*, *10*(8), 8. https://doi.org/10.3390/hydrology10080176

Krause, P., Boyle, D. P., & Bäse, F. (2005). Comparison of different efficiency criteria for hydrological model assessment. *Advances in Geosciences*, *5*, 89–97. Proceedings of the 8th Workshop for Large Scale Hydrological Modelling - Oppurg 2004 - 8th workshop for Large-scale hydrological modelling, Oppurg, Germany, 11–13 November 2004. https://doi.org/10.5194/adgeo-5-89-2005

Kumar, S., & Merwade, V. (2009). Impact of watershed subdivision and soil data resolution on ~~swat~~SWAT model calibration and parameter uncertainty. *JAWRA Journal of the American Water Resources Association*, *45*(5), 1179–1196. https://doi.org/10.1111/j.1752-1688.2009.00353.x

Kundu, D., Vervoort, R. W., & van Ogtrop, F. F. (2017). The value of remotely sensed surface soil moisture for model calibration using SWAT. *Hydrological Processes*, *31*(15), 2764–2780. https://doi.org/10.1002/hyp.11219

López López, P., Sutanudjaja, E. H., Schellekens, J., Sterk, G., & Bierkens, M. F. P. (2017). Calibration of a large-scale hydrological model using satellite-based soil moisture and evapotranspiration products. *Hydrology and Earth System Sciences*, *21*(6), 3125–3144. https://doi.org/10.5194/hess-21-3125-2017

Lyon, S. W., Walter, M. T., Gérard-Marchant, P., & Steenhuis, T. S. (2004). Using a topographic index to distribute variable source area runoff predicted with the SCS curve-number equation. *Hydrological Processes*, *18*(15), 2757–2771. https://doi.org/10.1002/hyp.1494

Mladenova, I. E., Bolten, J. D., Crow, W., Sazib, N., & Reynolds, C. (2020). Agricultural drought monitoring via the assimilation of SMAP soil moisture retrievals into a global soil water balance model. *Frontiers in Big Data, 3*, 10. https://doi.org/10.1109/JSTARS.2019.2923555

Mascaro, G., Vivoni, E. R., & Deidda, R. (2011). Soil moisture downscaling across climate regions and its emergent properties. *Journal of Geophysical Research: Atmospheres*, *116*(D22). https://doi.org/10.1029/2011JD016231

Mei, Y., Mai, J., Do, H. X., Gronewold, A., Reeves, H., Eberts, S., Niswonger, R., Regan, R. S., & Hunt, R. J. (2023). Can hydrological models benefit from using global soil moisture, evapotranspiration, and runoff products as calibration targets? *Water Resources Research*, *59*(2), e2022WR032064. https://doi.org/10.1029/2022WR032064

~~Moore, C., & Doherty, J. (2005). Role of the calibration process in reducing model predictive error. *Water Resources Research*, *41*(5). https://doi.org/10.1029/2004WR003501~~

Moriasi, D. N., Arnold, J. G., Van Liew, M. W., Bingner, R. L., Harmel, R. D., & Veith, T. L. (2007). Model evaluation guidelines for systematic quantification of accuracy in watershed simulations. *Transactions of the ASABE*, *50*(3), 885–900.

Mullen, K. M., Ardia, D., Gil, D. L., Windover, D., & Cline, J. (2011). DEoptim: An r package for global optimization by differential evolution. *Journal of Statistical Software*, *40*, 1–26. https://doi.org/10.18637/jss.v040.i06

~~Nanda, A., Jalilvand, E., Das, N. N., Bindlish, R., & Andreadis, K. (2023). *Optimizing Hydrologic Model Soil Physical Properties with Smap Soil Moisture: A Pathway for Skillful Assessment of Streamflow and Drought*. https://doi.org/10.2139/ssrn.4635449~~

Nanda, A., Jalilvand, E., Das, N. N., Bindlish, R., and Andreadis, K.: Optimizing hydrologic model soil physical properties with SMAP soil moisture: A pathway for skillful assessment of streamflow and drought, SSRN Electronic Journal [preprint], https://doi.org/10.2139/ssrn.4635449, 2023.

Nash, J. E., & Sutcliffe, J. V. (1970). River flow forecasting through conceptual models part I — A discussion of principles. *Journal of Hydrology*, *10*(3), 282–290. https://doi.org/10.1016/0022-1694(70)90255-6

Nathan, R. J., & McMahon, T. A. (1990). Evaluation of automated techniques for base flow and recession analyses. *Water Resources Research*, *26*(7), 1465–1473. https://doi.org/10.1029/WR026i007p01465

Nayeb Yazdi, M., Ketabchy, M., Sample, D. J., Scott, D., & Liao, H. (2019). An evaluation of HSPF and SWMM for simulating streamflow regimes in an urban watershed. *Environmental Modelling & Software*, *118*, 211–225. https://doi.org/10.1016/j.envsoft.2019.05.008

~~Neitsch, S. L., Arnold, J. G., Kiniry, J. R., & Williams, J. R. (2009). *Soil and water assessment tool theoretical documentation*. version 2009.~~

Neitsch, S. L., Arnold, J. G., Kiniry, J. R., and Williams, J. R. (2009) Soil and Water Assessment Tool theoretical documentation, Version 2009, Texas Water Resources Institute, Texas A&M University System, College Station, Texas, USA, available at: https://swat.tamu.edu/docs/ (last access: 4 August 2026), 2009.

O'Neill, P. E., Chan, S., Njoku, E. G., Jackson, T., Bindlish, R., & Chaubell, J. (2018). SMAP L3 radiometer global daily 36 km EASE-grid soil moisture, Version 5. *Natl. Snow Ice Data Cent*, 1–82.

O'Neill, P. E., Chan, S., Njoku, E. G., Jackson, T., Bindlish, R., Chaubell, J., & Colliander, A. (2023). SMAP e~~E~~nhanced L3 r~~R~~adiometer g~~G~~lobal and p~~P~~olar g~~G~~rid d~~D~~aily 9 km EASE-Grid Soil Moisture. *Boulder, Colorado, USA: NASA ~~Nafional~~National Snow and Ice Data Center Distributed ~~Acfive~~Active Archive Center*.

~~Parece, T., Dibetitto, S., Sprague, T., & Younos, T. (2010). *The Stroubles Creek Watershed: History of Development and Chronicles of Research.*~~

Parece, T., Dibetitto, S., Sprague, T., and Younos, T. (2010). The Stroubles Creek Watershed: History of development and chronicles of research, Water Resources Research Center, Virginia Tech, Blacksburg, VA, USA, 2010.

Patil, A., & Ramsankaran, R. (2017). Improving streamflow simulations and forecasting performance of SWAT model by assimilating remotely sensed soil moisture observations. *Journal of Hydrology*, *555*, 683–696. https://doi.org/10.1016/j.jhydrol.2017.10.058

Pechlivanidis, I. G., Jackson, B. M., McI~~i~~ntyre, N. R., & Wheater, H. S. (2011). Catchment scale hydrological modelling: A review of model types, calibration approaches and uncertainty analysis methods in the context of recent developments in technology and applications. *Global Nest Journal*, *13*(3), 193–214.

Peng, Y., Yang, Z., Zhang, Z., & Huang, J. (2024). A machine learning-based high-resolution soil moisture mapping and spatial–temporal analysis: The mlhrsm p~~P~~ackage. *Agronomy*, *14*(3), 3. https://doi.org/10.3390/agronomy14030421

Rajib, M. A., & Merwade, V. (2016). Improving soil moisture accounting and streamflow prediction in SWAT by incorporating a modified time-dependent Curve Number method. *Hydrological Processes*, *30*(4), 603–624. https://doi.org/10.1002/hyp.10639

Rajib, M. A., Merwade, V., & Yu, Z. (2016). Multi-objective calibration of a hydrologic model using spatially distributed remotely sensed/in-situ soil moisture. *Journal of Hydrology*, *536*, 192–207. https://doi.org/10.1016/j.jhydrol.2016.02.037

Sanford, W. E., Nelms, D. L., Pope, J. P., & Selnick, D. L. (2012). Quantifying components of the hydrologic cycle in Virginia using chemical hydrograph separation and multiple regression analysis. I~~n~~ *Scientific Investigations Report* (2011–5198). U.S. Geological Survey. https://doi.org/10.3133/sir20115198

Silvestro, F., Gabellani, S., Rudari, R., Delogu, F., Laiolo, P., & Boni, G. (2015). Uncertainty reduction and parameter estimation of a distributed hydrological model with ground and remote-sensing data. *Hydrology and Earth System Sciences*, *19*(4), 1727–1751. https://doi.org/10.5194/hess-19-1727-2015

S~~un, L. (2016). *Streamflow and soil moisture assimilation in the swat model using the extended kalman filter*. https://doi.org/10.20381/RUOR-4934~~

Sun, L.: Streamflow and Soil moisture assimilation in the SWAT model using the extended Kalman filter, PhD dissertation, University of Regina, Regina, Saskatchewan, Canada, https://doi.org/10.20381/RUOR-4934, 2016.

Thilakarathne, M., Sridhar, V., & Karthikeyan, R. (2018). Spatially explicit pollutant load-integrated in-stream *E. coli* concentration modeling in a mixed land-use catchment. *Water Research*, *144*, 87–103. https://doi.org/10.1016/j.watres.2018.07.021

Vereecken, H., Huisman, J. A., Hendricks Franssen, H. J., Brüggemann, N., Bogena, H. R., Kollet, S., Javaux, M., van der Kruk, J., & Vanderborght, J. (2015). Soil hydrology: Recent methodological advances, challenges, and perspectives. *Water Resources Research*, *51*(4), 2616–2633. https://doi.org/10.1002/2014WR016852

Wagner, W., Blöschl, G., Pampaloni, P., Calvet, J.-C., Bizzarri, B., Wigneron, J.-P., & Kerr, Y. (2007). Operational readiness of microwave remote sensing of soil moisture for hydrologic applications. *Hydrology Research*, *38*(1), 1–20.

Wagner, W., Lemoine, G., & Rott, H. (1999). A method for estimating soil moisture from ERS s~~S~~catterometer and s~~S~~oil d~~D~~ata. *Remote Sensing of Environment*, *70*(2), 191–207. https://doi.org/10.1016/S0034-4257(99)00036-X

Wakigari, S. A., & Leconte, R. (2023). Exploring the utility of the downscaled SMAP soil moisture products in improving streamflow simulation. *Journal of Hydrology: Regional Studies*, *47*, 101380. https://doi.org/10.1016/j.ejrh.2023.101380

Xu, Y., Cai, S., Huang, J., Liu, J., Shang, J., Yang, Z., & Zhang, Z. (2025). A multimodal deep learning approach for soil moisture downscaling using remote sensing and weather data. *Journal of Geophysical Research: Machine Learning and Computation,* 2(3), e2025JH000639. https://doi.org/10.1029/2025JH000639

Zeileis, A., Grothendieck, G., Ryan, J. A., Ulrich, J. M., & Andrews, F. (2025). *zoo: S3 Infrastructure for Regular and Irregular Time Series (Z's Ordered Observations)* (Version 1.8-14). https://cran.r-project.org/web/packages/zoo/index.html